Interim Technical Report
AFSWP - 868
August 1956

THE CHARRING OF WOOD DURING EXPOSURE TO THERMAL RADIATION

CORRELATION ANALYSIS FOR SEMI-INFINITE SOLIDS

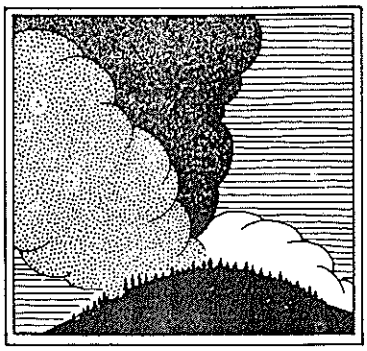

DIVISION OF FIRE RESEARCH
FOREST SERVICE
U. S. DEPARTMENT OF AGRICULTURE

ACKNOWLEDGMENTS

This study is part of a cooperative research program, sponsored by the Armed Forces Special Weapons Project, between the U. S. Naval Radiological Defense Laboratory and the Special Defense Project, California Forest and Range Experiment Station.

The author wishes to acknowledge the support of C. P. Butler and S. B. Martin of the Naval Radiological Defense Laboratory, particularly in answering numerous questions regarding their data. Thanks are also due Dr. A. F. Robertson of the National Bureau of Standards for supplying results from original data books, and to T. I. Monahan for providing information with reference to Naval Material Laboratory data.

Agriculture--Forest Service, Berkeley, Calif.

THE CHARRING OF WOOD

DURING EXPOSURE TO THERMAL RADIATION

Correlation Analysis for Semi-Infinite Solids

By

F. M. Sauer

Interim Technical Report AFSWP-868
August 1956

U. S. Department of Agriculture
Forest Service
Division of Fire Research
Washington, D. C.
A. A. Brown, Division Chief

Project Leader: W. L. Fons
California Forest and Range Experiment Station
P. O. Box 245
Berkeley, California

ABSTRACT

Available data on the behavior of wood undergoing charring and weight loss are summarized, both for isothermal heating and exposure to radiant energy. On the basis that measured temperatures during radiant heating behave as predicted by opaque semi-infinite solid theory and that thermal degradation of wood is governed by a first order kinetic reaction, a differential equation is postulated for the charring process. Schematic integration of this equation yields dimensionless groups which are independent of a "charring temperature." Analysis of Naval Radiological Defense Laboratory data leads to the conclusion that during radiant exposure the charring process is primarily controlled by the diffusion of heat into the interior of the solid, i.e., the effect of rate-controlling variables is small.

Comparison of NRDL square wave and field pulse data leads to the relationship for the equivalent square wave pulse: H (square wave) = 0.60 H_m (field pulse), t (square wave) = 4.0 t_m (second maximum). This relationship holds over the entire range of NRDL investigations within the confidence level of data, and provides a satisfactory check against National Bureau of Standards BUSTER field data.

Massachusetts Institute of Technology and NBS charring data are compared against the derived dimensionless correlations. These data yield char depths which are 25 percent lower than NRDL results. This differential is attributed to different heat flow directions relative to the grain of the wood. This conclusion, however, requires clarification through additional experimentation.

Naval Material Laboratory static exposure depth of char data show large relative scatter and appear to be influenced by the finite solid boundary. Dynamic exposure data yield correlations unlike those of square wave (static) exposures due to the pulse shape imposed by the method of exposure.

The presented correlations are believed directly applicable to a wide variety of woods other than those tested, provided these woods do not have a marked grain structure such as in Douglas fir. Exposure of the latter type of wood produces a corrugated effect due to the difference in density between spring and summer growth. The rate of charring in each case must then be treated separately.

The role of initial temperature is not delineated due to lack of significant variation in temperature and activation energy data. However, the effect of initial temperature is believed to be small since temperature enters the correlations as the absolute temperature (^{o}K). Also activation energies for most non-tropical woods appear to

be in the range of 30×10^3 cal/mole ± 10 percent. It is suggested that correlations be entered with $T_o = 300^oK$ for all initial temperatures within the range of $0\text{-}60^oC$.

Deviations from the proposed correlations are discussed in the light of finite solids and diathermancy effects. Recommendations are presented for future work which should answer questions arising from moisture, finite thickness, and diathermancy.

CONTENTS

TABLES

ILLUSTRATIONS

INTRODUCTION

General

The charring of surfaced wood during exposure to thermal radiation has been studied experimentally by a number of investigators during the past several years. Quantitative description of charring has usually involved specification of the depth to which charring has penetrated, i.e., the depth of char. In two instances associated loss of weight has been measured.

The significance of quantitative measurement of charring is not directly associated with the relative importance of charring as "damage." That is, charring will rarely constitute damage unless it has been so severe as to structurally weaken the wooden member. If such is the case, sustained ignition will most probably occur, and the subsequent damage enters the realm of fire rather than the realm of charring.

Knowledge of the mechanism of charring is significant, however, in three ways. First, depth of char may be used as a passive indicator of thermal yield and should provide useful corroborative evidence in most situations due to widespread use of wood as a structural and crating material.

Secondly, such knowledge is useful in providing a means of comparison of thermal damage produced by constant radiation intensity (square wave) pulses and field (weapon) pulses. In this case an"equivalent" square wave pulse may be specified which may allow conversion of a large quantity of thermal damage data obtained in the laboratory using square wave pulses. In the same category one may place comparison of damage produced by different laboratory sources.

Thirdly, depth of char and weight loss data provide valuable information on those mechanisms which precede ignition and which occur during combustion of wood. Consequently these data provide a fundamental insight into these mechanisms. It is for this reason that these data are of particular interest to the author.

Underlying the above applications there appears a set of fundamental questions which must be answered. First, what is the role of thermal properties of the material and how are they grouped? What is the effect of irradiance level and exposure time, i.e., how does charring scale relative to weapon size? To what extent does the rate of thermal decomposition govern depth of char? How effective is moisture in retarding char? It is quite apparent that fundamental conclusions can be reached only through systematic correlation of all available charring data. Furthermore, data correlation should be based on dimensionless grouping of parameters or moduli which are consistent with theoretical concepts of heat conduction and thermal decomposition.

The purpose of this report is to present an analysis which leads to a series of dimensionless moduli and to derive empirically the relationships between them.

Historical

Depth of char measurements have been made on two species of wood during Operation BUSTER, and are reported by Robertson of the National Bureau of Standards (1,2).[1/] Laboratory measurements on several different species of wood exposed under conditions of constant irradiation have been reported by the NBS (2,3,4), the U. S. Naval Materials Laboratory (5,6), and by Williams of the Massachusetts Institute of Technology (7). Corresponding weight loss measurements have been made by the NBS (4,8). Depth of char and associated weight loss have been investigated by Martin, Butler and Plum of the U. S. Naval Radiological Defense Laboratory (9) after exposure to both constant irradiance and a simulated (laboratory) field pulse. The NRDL data represent the most extensive of those reported as to irradiance level, pulse time, and pulse shape although this investigation was made on a single species of wood.

In each of these investigations thermal sources of different characteristics were used and in general the detailed method used to measure char depth varied. Methods of measurement will be discussed in detail in a later section.

Correlation of depth of char during constant irradiation has been proposed by Williams (7) and Masters (10). Both correlation procedures utilize dimensionless groupings based on heat conduction theory which requires specification of the "temperature at which incipient char occurs." Williams bases his analysis on the temperature profile occurring at the termination of the square wave exposure. Masters considers as a criterion the maximum temperature rise due to a square wave pulse as derived previously by Lauwerier (11). Both analyses consider the wood specimen to be a homogeneous, semi-infinite, opaque, inert solid. Heat losses due to convection and/or back radiation were not considered.

While the latter postulates may be quite necessary from a theoretical point of view, the imposition of a charring temperature does not conform to our present knowledge of the mechanism of charring which indicates that thermal decomposition is a time-dependent as well as temperature-dependent phenomenon. This deficiency in analysis is exemplified by the necessity of using different "charring temperatures" for each set of data analyzed. Furthermore, it is difficult to conceive a description of weight loss based on temperature alone.

1/ Numbers in parentheses refer to Literature Cited, page 66.

THERMAL DECOMPOSITION OF WOOD

The concept of thermal decomposition as a kinetic reaction has been employed successfully by Bamford, Crank and Malan (12) in the mathematical treatment of the ignition process. Thermal decomposition was treated as a first order kinetic reaction, i.e.,[2]

$$\frac{dw}{d\theta} = -\mu w \exp\left(-\frac{E}{RT}\right) \qquad (1)$$

While these theoretical results were not extensive enough to describe the complete system the results show excellent agreement with experimental data on ignition and charring reported in the same paper. Thus it appears that treatment of decomposition as a first order reaction is an adequate and necessary element in theoretical treatment of thermal damage.

The thermal decomposition of wood during heating in a constant temperature environment has been studied by McNaughton (13), Wright and Hayward (14), Stamm, Burr and Kline (15), and MacLean (16,17,18,19). Mitchell, Seborg and Millet (20) have investigated decomposition of wood derivatives. Thermal decomposition rates for paper and other electrical insulating materials are reported by Kujirai and Akahira (21), and Murphy (22). These studies indicate that rate of weight loss, production of gases, and loss of strength are time-dependent as well as temperature-dependent quantities. MacLean (16) investigated a number of hardwoods and soft woods, and found that hardwoods disintegrate more rapidly than soft woods, presumably because of higher hemicellulose and lower lignin content, although the difference was not marked. He also concludes (19) that the effect of moisture would increase hydrolysis of the wood components and hasten deterioration. Increased humidity of the surrounding air has the same effect. For both hardwoods and soft wood he observed that when weight loss was from 35 to 45 percent of the original oven-dry weight the samples "were well charred and could be easily broken or crumbled by hand."

The increased rate of decomposition due to moisture is also found in the data of Mitchell, et al. Samples heated in closed containers lost weight much more rapidly than those flushed with small amounts of air to remove the water vapor resulting from decomposition. These data also show very similar weight loss when sawdust was heated in a circulating air and nitrogen atmosphere indicating that weight loss was substantially due to decomposition rather than oxidation although the presence of oxygen increases the amount of products produced.

2/ See Nomenclature, page 70.

When the time of heating is long compared to the time required for the sample temperature to reach equilibrium with the environment the process may be considered, without serious error, to be entirely a constant temperature process within the wood. Equation (1), integrated at constant temperature, becomes

$$\ln w = - \mu\theta \exp(- \frac{E}{RT}) \tag{2}$$

The total weight of gas produced by decomposition is not equal to the total dry weight of wood substance. The data quoted by Klar (23) and Blanchard (24) indicate the weight fraction of inert material to dry wood, f, to be in the order of 15 percent under nonoxidizing conditions. This inert material is mostly carbon which will combust in the presence of oxygen provided the temperatures are sufficiently high. The ratio of weight to initial dry weight becomes

$$w_o = w(1 - f) + f \tag{3}$$

or

$$w = \frac{w_o - f}{1 - f} \tag{4}$$

Values of w were computed, using $f = 0.15$, from the data reported by McNaughton using equation (4) and are plotted as $-\ln w$ vs θ in figure 1.[3/] The linear relationship indicates that the temporal relationship of equation (2) is satisfied. Slopes of figure 1 for each temperature are plotted vs $1/T$ in figure 2. The linear relationship indicates that equation (2) describes the decomposition phenomenon, at least within the temperature range investigated.

Numerical values for the velocity constant and activation energy can be found from figure 2. These values (table 1) are seen to compare favorably with values used by Bamford, et al (12) to allow juxtaposition of their theoretical and experimental results.

Stamm (25) has examined a number of decomposition data (15,16,17, 18,19,20) on a similar kinetic reaction basis except that in the case of weight loss f was taken as zero. The results of Stamm, expressed as velocity constants and activation energies, and similar constants for various electrical insulating materials are also shown in table 1.

3/ These data are also corrected for initial moisture content (approximately 7 percent) as moisture can be assumed removed during the short heating period required to reach equilibrium temperature conditions.

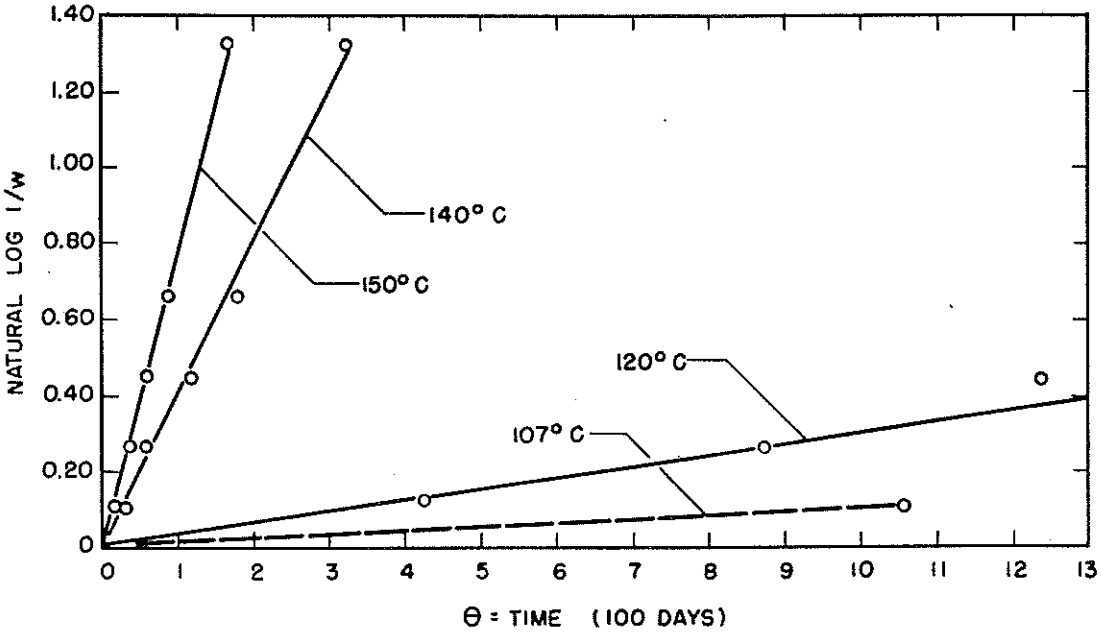

Figure 1.--Variation with time of weight fraction of decomposition products in hard maple (data of McNaughton)

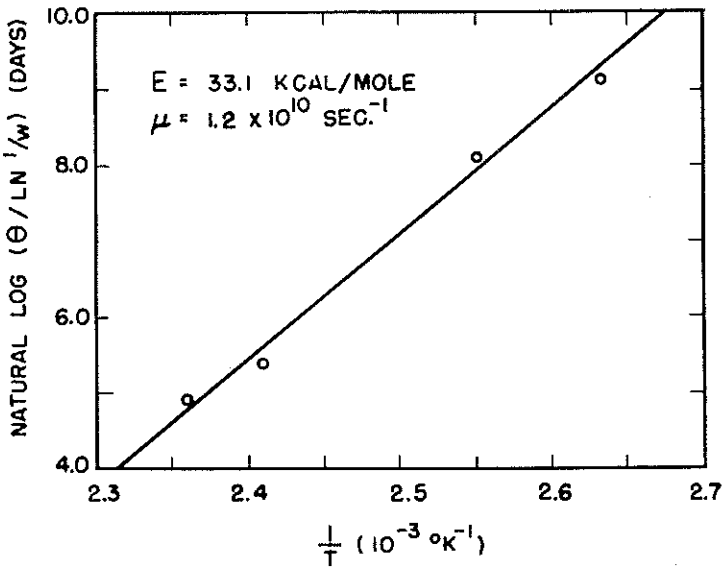

Figure 2.--Arrhenious plot for thermal degradation of hard maple (data of McNaughton)

Table 1.--Activation energies (E) and velocity constants (μ) for weight loss during thermal decomposition (oven heating)

Material	E kcal/mole	μ sec^{-1}	Temperature range °C	Ref.
Hard maple	1/ 33.1	1/ 1.2×10^{10}	107-150	13
Wood (species not identified)	33.2	5.3×10^{8}	2/ 30-530	12
Coniferous wood	29.5	5.1×10^{11}	93.5-250	25
Sitka spruce (under molten metal)	29.8	2.3×10^{11}	167-300	25
Douglas-fir sawdust	25.0	1.9×10^{9}	110-220	25
Alpha cellulose	26.0	4.8×10^{9}	110-220	25
Hemicellulose	26.7	3.6×10^{10}	110-220	25
Lignin	23.0	8.9×10^{7}	110-220	25
Cotton	32.1	1/ 1.3×10^{12}	165-265	21
Filter paper	31.0	1/ 7.5×10^{11}	165-265	21
Linen	31.0	1/ 4.5×10^{11}	165-265	21
Manila paper	31.7	1/ 2.8×10^{12}	145-265	21
Silk	32.7	1/ 5.9×10^{12}	125-265	21
Empire cloth 3/	25.5	1/ 3.8×10^{9}	105-265	21
Kraft and linen condenser paper	4/ 33.5	--	100-225	22

1/ Compiled by author from referenced data.
2/ Temperature range of theoretical analysis.
3/ Cotton cloth treated with linseed oil.
4/ For rate of gas evolution.

SUMMARY OF DATA

Property Values

Depth of char and weight loss measurements have been made on a variety of woods ranging in density from 0.16 to 0.73 gm/cc. In all cases exposures were made in the radial or tangential grain directions, i.e., no end grain (longitudinal) exposures were made. The range of variables and conditions of exposure are summarized in table 2.

Thermal conductivities and diffusivities were computed from corresponding densities using the relationship presented by MacLean (26)[4/]

$$k = \left[(4.78 + 0.097M)\rho_M + 0.57\right] \times 10^{-4} \quad ; \quad 0 < M < 40 \qquad (5)$$

and the average specific heat of dry wood from Dunlap (27). Specific heats for wood containing moisture were calculated using the method of Byram (28, p.13)

$$c = 0.33 + M + \Delta c_p \qquad (6)$$

where Δc_p represents the elevation of specific heat due to the heat of desorption of bound water. Densities were corrected for swelling or shrinkage using the relationship (31)

$$\rho_D = \frac{\rho_M}{1 + 0.009\ M\ \rho_M} \quad \text{and} \quad \rho_M = \frac{\rho_D}{1 + 0.009\ M\ \rho_D} \qquad (7)$$

4/ The conductivity-density relationships presented by MacLean refer to heat flow in the partly radial and partly tangential directions and appear accurate to ±5 percent. Earlier work by Wangaard (29) indicates that for hardwoods radial conductivity is 5 to 10 percent greater than tangential conductivity, whereas in soft woods differences were not detectable. This difference in hardwoods is attributed by Wangaard to the influence of the radially oriented wood rays. Ray volume in soft woods is so small that this differential influence is insignificant. Wangaard (30) has also studied the longitudinal conductivity of Douglas-fir and found that the ratio of longitudinal to transverse conductivity varies from 2.3 to 3.8 depending upon the fibril angle. Since conductivities along the grain appear several times the transverse value, specimens cut cross-grain, as is generally the case with commercially cut exotic woods showing no ring growth, may have thermal conductivities appreciably higher than indicated by equation (5) depending on the degree of cross grain present. Although data to the contrary are not apparent application of equation (5) to exotic species should be done with caution. Balsa, however, appears to correlate well with equation (5) (26).

Table 2.- Summary of exposure conditions and property values

Agency	Species	Density (dry) (gm/cc)	Moisture content (percent)	Irradiance (cal/cm²sec) max.	Irradiance (cal/cm²sec) min.	Exposure time (sec) max.	Exposure time (sec) min.	Depth of char (mm) max.	Depth of char (mm) min.	Initial temperature (°C)	Specimen thickness (inches)	Conductivity (10^{-4}cgs units) wet[1]	Conductivity (10^{-4}cgs units) dry[2]	$\sqrt{\text{Diffusivity}}$ (10^{-2}cgs units) wet	$\sqrt{\text{Diffusivity}}$ (10^{-2}cgs units) dry	$\frac{1}{\sqrt{k\rho c}}$ (cgs units) wet	$\frac{1}{\sqrt{k\rho c}}$ (cgs units) dry
Square Wave Exposures																	
NRDL(9)	Heart willow	0.44	7.5	24.9	2.5	30	0.34	4.71	0	25	1/4-1/2	2.9	2.7	3.9	4.3	130	160
MIT(7)	Ponderosa pine	0.38	0	3.5	2.4	40.4	21.2	3.9	1.4	40	(3/)	--	2.4	--	4.4	--	180
	Birch(sapwood)	0.59	0	3.5	2.4	38.5	34.2	3.3	2.4	40	(3/)	--	3.4	--	4.2	--	120
NBS(2)	Sugar pine	0.35	7	17.5	5.0	24.8	1.9	2.52	0.35	4/25	1/4	2.4	2.2	4.1	4.4	170	200
	Mahogany	0.50	7	17.5	5.0	24.8	1.9	2.40	0.37	4/25	1/4	3.2	3.0	3.9	4.2	120	140
	Hard maple	0.56	7	17.5	5.0	24.9	1.9	2.09	0.25	4/25	1/4	3.5	3.2	3.9	4.2	110	130
(8)	Sugar pine I	0.38	7/0	5/8.5	--	1.0	7.0	6/--	--	4/25	1/2	--	2.4	--	4.4	--	180
	Sugar pine II	0.39	7/0	5/8.5	--	1.0	7.0	6/--	--	4/25	1/2	--	2.4	--	4.4	--	180
	Sugar maple	0.49	7/0	5/8.5	--	1.0	7.0	6/--	--	4/25	1/2	--	2.9	--	4.2	--	140
NML(6)	White pine	8/0.39	7.4	85	--	0.76	0.10	1.6	0	4/25	1/4	2.7	2.4	4.0	4.4	150	180
	Maple	8/0.68	7.1	85	--	1.04	0.20	1.0	0	4/25	1/4	4.1	3.8	3.8	4.1	92	110
(5)	Hard maple (sapwood)	8/0.61	8.3	60	5	19	0.1	1.8	0	4/25	1/8	3.8	3.5	3.8	4.2	100	120
Field Pulse Exposures																	
NRDL(9)	9/Heart willow	0.44	7.5	25.4	6.3	6.51	0.13	3.85	0	25	1/4-1/2	2.9	2.7	3.9	4.3	130	160
NBS(2)	Balsa	10/0.16	11/--	74.7	22.4	0.16	0.12	1.87	0.42	12/12	1/2	--	1.3	--	5.0	--	380
	Mahogany	10/0.53	11/--	74.7	22.4	0.16	0.12	0.40	0.08	12/12	1/2	--	3.1	--	4.2	--	140

1/ Computed at prevailing moisture content
2/ Computed at zero moisture content
3/ Not reported
4/ Assumed
5/ Increased from 7 cal/cm²sec as reported in (4) (private communication from A. F. Robertson dated March 16, 1954)
6/ Weight loss only
7/ Assumed; original data not clear
8/ Reported densities corrected for moisture and shrinkage (private communication from Thomas I. Monahan dated November 18, 1952)
9/ Simulated (laboratory) field pulse data
10/ Roeser, W. F. Tenth progress report on effects of thermal radiation on materials, AFSWP-279, Natl. Bur. Stds., 1952
11/ Unknown
12/ Shot-time ambient temperature (Gilbert, H. K., and Wilson, R. Q. Operation BUSTER Final Report, WT-412, 1952)

Thermal conductivity, diffusivity, and $\sqrt{kpc}$ were computed from the above equations on the basis of prevailing moisture content and on a dry basis. Values used throughout the analysis are displayed in table 2.

Depth of Char Measurement Techniques

"Depth of char" represents a relative measurement at best since charring is a progressive process and char depths reported under identical exposure conditions are apt to vary between experimenters. The degree to which an experimental technique is related to another is most difficult to assess. This in itself is a factor which must not be overlooked.

NRDL measurements (31,p.23) were made by brushing samples with a stiff nylon-bristled brush to remove all loose char. Char depth was then measured with a dial indicator. Reported values represent the mean of 7 or 8 determinations. Standard deviations are also reported.

NML char depths were determined by sectioning the specimen after exposure; then with a traveling microscope, measurements were made of the distance from the unexposed surface to the "point of deepest char." Data are reported only in graphical form and statistical measures are not quoted. NML data on hard maple sapwood (5), as reported, are the result of cross plotting, since curves of uniform depth increments are presented. This in itself seriously reduces the applicability of these results.

Two values for depth of char are presented by the MIT measurements. One value corresponds to the "easily discernible transition from the black 'complete charred' condition to one that is only a dark brown." The second value represents "the farthest depth of penetration for any discoloration of the natural wood." Measurements were probably made by optical means although the technique is not reported. Data on single determinations are reported.

Laboratory determinations of char depth reported by the NBS were determined by sanding down the specimens until "char was just removed." Data on individual tests are reported. Field data were determined by sectioning the sample and measuring the depth "to the bottom of the charred layer" with a traveling microscope and/or by optical projection. Reported values are the average of the two methods for several specimens exposed at the same station.

Weight Loss Measurement Techniques

Samples exposed by NRDL were equilibrated at 43 percent relative humidity (7.5 percent moisture), weighed, exposed, and returned to the humidity chamber for at least 2 hours before final weight was

determined. Weighing was done prior to removal of char and presumably at the original moisture content. Data are averages for 7 or 8 determinations.

NBS weight loss was determined from before and after weighings. Reconditioning was unnecessary since samples were exposed oven dry. Data on single determinations are reported.

DERIVATION OF DIMENSIONLESS GROUPINGS OF PARAMETERS

General

Before carrying out derivation of the dimensionless moduli it is perhaps worth while to discuss available information concerning the behavior of wood during exposure to thermal radiation. The reader will recognize the extreme complexity of an "exact" solution to the problem of charring and weight loss. First, wood is not isotropic with reference to its thermal properties and is not generally homogeneous along its principal axis due to variation in density between spring and summer growth. During irradiation, surface absorptance and diathermancy vary with respect to the degree of surface charring, and as the wood undergoes decomposition its density and thermal conductivity likewise change their magnitude.

A rigorous theoretical solution of the charring process would require consideration of these variations of thermal properties with temperature, degree of degradation and moisture, chemical oxidation reactions, attenuation of radiant flux by smoke, convective and reradiation heat losses, movement inward of the exposed surface due to charring, and other extremely complex boundary conditions. Fortunately the behavior of wood appears to follow quite closely the most simple theoretical postulate for temperature variation, i.e., the opaque, constant property, semi-infinite solid neglecting heat losses and chemical reactions (32,p.56).

Little is known of the precise state of charcoal formed under various rates of heating. Available data, however, suggest that the diffusivity of charcoal is of the same order of magnitude as that of the original wood, although individual values of density, conductivity and specific heat are variable. This suggests that an assumption of constant thermal properties may be a much better approximation than appears at first sight.

Measured temperature distributions in oven-dried wood specimens during irradiation by a 2000°K source (graphite resistance furnace) have been correlated within the scatter of data by Williams (7,p.72) against the opaque semi-infinite solid solution. Williams remarks that "the absence of any diathermancy effect is somewhat surprising."

Gardon's temperature measurements (33) using a solar source suggest, however, that wood is diathermanous to at least a portion of this shorter wave length radiation. When the wood surface was blackened with india ink results agree closely with the opaque solid solution. Thus diathermancy appears to be of secondary importance and may be considered as a perturbation.

Temperature measurements in moist (10-13 percent moisture content) and green (212-230 percent moisture content) wood samples are also correlated with the opaque solid solution by Williams (7,p.77-86) within a maximum deviation of 40-50 percent, provided the specific heat is increased in the amount suggested by Byram (28) to account for the heat of desorption. The fact that moisture apparently does not act as a heat sink (due to the heat of vaporization) in the interior of the wood is ascribed by Williams to be the result of rearward migration and subsequent condensation of water vapor.

Successful correlation of heat and mass transfer data in similar, but usually less complex, problems generally follows a methodology which first involves specification in mathematical terms, viz., a differential equation, the known or postulated behavior of the phenomenon under study. A relatively limited number of "classical" equations may be considered rigorous in this respect. One must usually work with a simplified model of the process which, however, must contain the major fundamental aspects under consideration. Certain further simplifications may be mathematically necessary to obtain a formal solution or to set up the problem for computation techniques.

The final product rarely results in exact numerical magnitudes when compared with data; it does however define dimensionless groupings of parameters and their relative influence, orders of magnitude, and expected trends. This information is of great importance to the experimenter in that he may predetermine the range of interest of variables and accuracy desired, and correctly schedule testing so that data are uniformly distributed over the range of interest. The data analyst may now apply correlation procedures which are theoretically sound. He must at times, however, use empirical procedures to correct for deficiencies in the original analysis, especially in the often occurring case where thermal properties vary during the process due to extreme variation of temperature or concentration, cf., Williams' treatment of moisture in wood during irradiation (7,p.77).

The derivation of dimensionless groups or moduli does not require formal solution of the postulated equations. Moduli may be found by the procedure of dimensional analysis, or more rigorously from the dimensionless form of the differential equation(s), or by symbolic integration of the equation(s). The latter procedure will be used in the next section to define those groupings relating to charring and weight loss.

Specification of Dimensionless Moduli for Square Wave Exposure

The fundamental postulate involved in the following derivation is that "charring" occurs when the density is reduced sufficiently by degradation, or more specifically when the ratio of density to original density reaches a given value. This definition is in conformance with the findings of MacLean (19); however, since "charring" is a question of degree, this density ratio may vary between investigators due to the specific method of determining "depth of char."

Since the weight loss during degradation follows a first order kinetic reaction, a reasonable assumption is that density changes, occurring at a fixed position, x, within the solid, may be represented in a like manner, viz.,

$$-\frac{1}{\rho}\left(\frac{\partial \rho}{\partial \theta}\right)_x = \mu \exp\left(-\frac{E}{RT}\right) \tag{8}$$

Since volume changes of samples heated at constant temperature appear relatively minor, the constants μ and E should be approximately those for weight loss (table 1). The influence of a non-zero value for f, equation (3), appears relatively minor provided f is small and large density changes are not considered.

Equation (8) is presented graphically in figure 3 using the velocity constants and activation energies determined by Stamm (25) for coniferous wood and Sitka spruce. The former constants hold for wood under oxidizing conditions while the latter are for non-oxidizing conditions. The data of McNaughton are not presented since the rather large extrapolation in temperature range is not justified.

The temporal variation of temperature at position, x, during a square wave exposure may be approximated by the theoretical solution for the opaque semi-infinite solid. For the boundary conditions that

$$-k\frac{\partial T}{\partial x} = \alpha H \ , \quad 0 \leqslant \theta \leqslant t$$

$$-k\frac{\partial T}{\partial x} = 0 \ , \quad t \leqslant \theta$$

This solution may be written as (32, p. 57)

$$\left.\begin{aligned} \frac{\Delta T k}{\alpha H x} &= \frac{1}{\eta}\ \text{ierfc}\ \eta \ , \quad 0 < \frac{1}{\eta} \leqslant \frac{1}{\eta_2} \\ &= \frac{1}{\eta}\ \text{ierfc}\ \eta - \frac{1}{\eta_1}\ \text{ierfc}\ \eta_1 \ , \quad \frac{1}{\eta_2} \leqslant \frac{1}{\eta} \end{aligned}\right\} \tag{9}$$

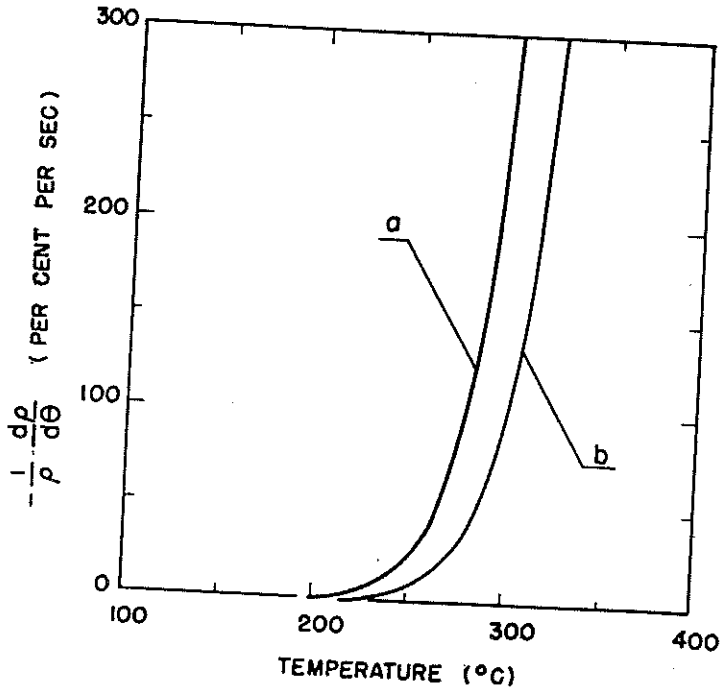

Figure 3.--Variation with temperature of time rate of density change (a, coniferous wood heated in air; b, Sitka spruce heated under molten metal)

where $\eta = \frac{2}{2\sqrt{a\theta}}$, $\eta_1 = \frac{x}{2\sqrt{a(\theta-t)}}$, and $\eta_2 = \frac{x}{2\sqrt{at}}$

The dimensionless temperature rise is then a function of the two parameters η and η_1

$$\frac{\Delta Tk}{\alpha Hx} = F_o(\eta_1,\eta) \qquad (10)$$

or since $\frac{1}{\eta_1^2} = \frac{1}{\eta^2} - \frac{1}{\eta_2^2}$ then

$$\frac{\Delta Tk}{\alpha Hx} = F_1(\eta_2,\eta) \qquad (11)$$

Equation (8) may now be written in dimensionless form, after introducing equation (11), as

$$\frac{1}{\rho^+}\left(\frac{\partial \rho^+}{\partial \eta}\right)_{x^+} = \mu^+ \eta^{-3} \exp\left[-E^+ F_2(x^+, \eta_2, \eta)\right] \tag{12}$$

where $\rho^+ = \frac{\rho}{\rho_o}$, $\mu^+ = \frac{\mu x^2}{2a}$, $E^+ = \frac{E}{RT_o}$, $x^+ = \frac{\alpha H x}{kT_o}$ and $F_2 = \left[1 + x^+ F_1(\eta_2, \eta)\right]^{-1}$. Integrating equation (12) we obtain the density distribution as a function of time, η

$$\int_1^{\rho^+} \left(\frac{\partial \rho^+}{\rho^+}\right)_{x^+} = \mu^+ \int_\infty^\eta \exp\left[-E^+ F_2(x^+, \eta_2, \eta)\right] \eta^{-3} \, d\eta \tag{13a}$$

$$\ln \rho^+ = F_3(\mu^+, E^+, x^+, \eta_2, \eta) \tag{13b}$$

where ρ^+ is now the density variation at constant x^+.

Incipient charring is assumed to occur at a particular value of ρ^+, say B. At large times after exposure, sufficient for the temperature profile to decay, i.e., $\eta \longrightarrow o$, the density ratio B appears at x equal to the depth of char, d. Hence after exposure we have

$$\ln \rho^+ = F_3(\mu^+, E^+, x^+, \eta_2, 0) \tag{13c}$$

hence

$$\ln B = F_3(\mu^+, E^+, x^+, \eta_2, 0); \quad [x = d] \tag{13d}$$

The correlation equation then assumes the form (since B is a constant)

$$\frac{\alpha H d}{kT_o} = F_4\left(\frac{d}{\sqrt{at}}, \frac{\mu d^2}{a}, \frac{E}{RT_o}\right) \tag{14}$$

or any number of alternate forms generated by multiplication of powers of two or more variables, i.e.,

$$\frac{\alpha H d}{kT_o} = F_5\left(\frac{\alpha H \sqrt{t}}{T_o \sqrt{k\rho_c}}, \frac{\mu d^2}{a}, \frac{E}{RT_o}\right)$$

$$\frac{d}{\sqrt{at}} = F_6\left(\frac{\alpha H\sqrt{t}}{T_o\sqrt{k\rho c}} \ , \ \mu t \ , \ \frac{E}{RT_o}\right)$$

and others.

It is desirable to change the form of equation (13c) in a like manner so that x appears in only one of the variables, viz., η_2.

$$\ln \rho^+ = F_7 \ (\mu t \ , \ E^+ \ , \ H^+ \ , \ \eta_2) \tag{15}$$

where $H^+ = \frac{\alpha H\sqrt{t}}{T_o\sqrt{k\rho c}}$. The change in weight ΔW , resulting from the density distribution of equation (15) is

$$\Delta W = A\rho_o \int_o^\infty (1-\rho^+)dx \tag{16}$$

or

$$\frac{\Delta W}{\rho_o A\sqrt{at}} = \int_o^\infty \left[1 - e^{F_7(\mu t \ , \ E^+ \ , \ H^+ \ , \ \eta_2)}\right] d\eta_2 \tag{17}$$

resulting in a correlation equation for weight loss

$$\frac{\Delta W}{\rho_o A\sqrt{at}} = F_8\left(\frac{\alpha H\sqrt{t}}{T_o\sqrt{k\rho c}} \ , \ \mu t \ , \ \frac{E}{RT_o}\right) \tag{18}$$

or other alternate forms.

At this point, for the purpose of consolidating analytical material, we anticipate ourselves and inquire into the groupings which portray the behavior of a slightly diathermanous material. For materials which exhibit an absorption coefficient β , independent of wave length, there is introduced another grouping $\beta\sqrt{at}$ or βx (7,p.23). For wood β does not appear to be a true constant (34). However, since wood appears only slightly diathermanous, it is reasonable to assume β is a constant, which may be determined empirically, and to treat diathermancy as a perturbation upon the opaque solid.

The maximum surface temperature rise of an opaque solid is a function of the irradiance modulus $\frac{\alpha H\sqrt{t}}{T_o\sqrt{k\rho c}}$, viz.,

$$\frac{(\Delta T_o)_{max}}{T_o} = \frac{2}{\sqrt{\pi}} \cdot \frac{\alpha H\sqrt{t}}{T_o\sqrt{k\rho c}} \tag{19}$$

Similarly, the maximum surface temperature rise of a diathermanous solid is given by the expression (33,p.14)

$$\frac{(\Delta T_o)_{max}}{T_o} = \frac{2}{\sqrt{\pi}} \cdot \frac{\alpha H\sqrt{t}}{T_o\sqrt{k\rho c}} F(\beta\sqrt{at}) \tag{20}$$

where $$F(\beta\sqrt{at}) = 1 - \frac{\sqrt{\pi}}{2\beta\sqrt{at}}\left[1 - e^{\beta^2 at}\ \mathrm{erfc}\ (\beta\sqrt{at})\right] \tag{21}$$

The function $F(\beta\sqrt{at})$ is shown graphically in figure 4. The surface temperature rise of the diathermanous solid is seen to approach that of the opaque solid as time increases. $F(\beta\sqrt{at})$ assumes the limiting forms for large and small times

$$F(\beta\sqrt{at}) = 1 - \frac{\sqrt{\pi}}{2\beta\sqrt{at}}, \quad 50 < \beta\sqrt{at} \tag{22}$$

$$F(\beta\sqrt{at}) = \frac{\sqrt{\pi}}{2}\beta\sqrt{at}, \quad \beta\sqrt{at} < 0.05 \tag{23}$$

From a strictly empirical standpoint, the irradiance modulus as originally derived is replaced by the more general expression $\frac{\alpha H\sqrt{t}}{T_o\sqrt{k\rho c}} \times F(\beta\sqrt{at})$.

Field Pulse Exposures

An identical analysis will lead to the correlation functions for the field pulse with H replaced by H_m (the maximum flux) and t replaced by t_m (time of the second maximum). The relationships will obviously be numerically different although their behavior should be very similar.

CORRELATION OF DATA

Selection of Dimensionless Moduli

Since it appears, at the onset, that the depth of char $\frac{Hd}{kT_o}$ and weight loss $\frac{\Delta W}{\rho_o A\sqrt{at}}$ moduli are at least a function of three other dimensionless moduli, a short discussion of the significance of these

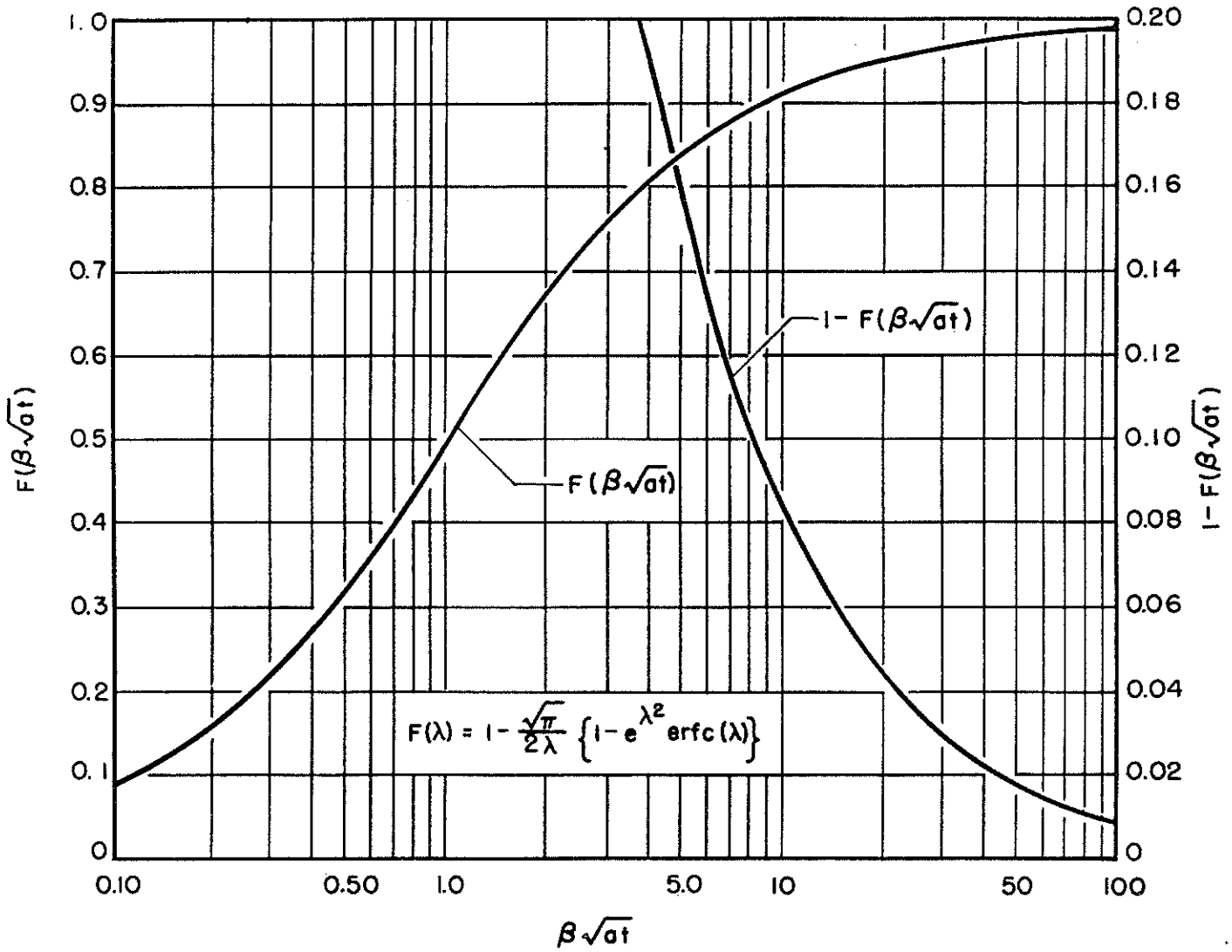

Figure 4.--Surface temperature correction due to diathermancy, $F(\beta\sqrt{at})$

parameters will simplify their application to the experimental data. Notice that the moduli do not contain a "charring temperature." This is of course a result of the introduction of the rate equation, equation (8), and the postulate that charring occurs at a particular (but unknown) value of the density ratio, $\rho^* = B$.

First the data analyst has at his disposal a series of alternate groupings of these moduli which he may choose in order to best correlate the data at hand. These moduli fall into two general categories of significance, those which govern the behavior in terms of the chemical reactivity, i.e., μt and $\frac{E}{RT_o}$, and those which pertain to the diffusion of temperature into the interior of the solid. Since the velocity of propagation inwards (of the depth of char) is associated with large temperature gradients, the process may be controlled during the transient phase either by the chemical reaction rate (rate controlled) or by the temperature gradients themselves (diffusion controlled). The steady state condition, i.e., the velocity of propagation becomes constant, is brought about by mutual interaction between an endothermic charring reaction, heat losses, and energy supplies through conduction.[5] Under such conditions the process may be considered either rate- or diffusion-controlled. Such is the case during combustion of liquid fuels (35) and during the high temperature reaction of graphite with carbon dioxide (36).

Intuitively, continuous exposure of an infinitely thick solid should eventually result in steady state since if the velocity of propagation were to continuously decrease, the absurd situation finally results that additional charring ceases to occur perceptibly. If the velocity were to increase, ad infinitum, one would suspect a substantial exothermic reaction within the interior of the semi-infinite solid which is contrary to the findings of Byram (28) and Robertson (4). This is not to be confused with the exothermic oxidation (combustion) reaction which takes place adjacent the surface during flaming or glowing.

Selection of moduli is then concerned primarily with correlation during the transient phase. Groupings chosen representative of rate-controlled process should, by suitable multiplication of groups, be

---

[5] Steady state does not occur, in this sense, during isothermal degradation since temperature gradients are small leading to a completely rate-controlled process.

independent of thermal conductivity. The author has preferred to use the following forms of equations (14) and (18) which appear suitable for diffusion-controlled charring and weight loss[6]

$$\left.\begin{aligned} \frac{\alpha H d}{kT_o} &= G_o\left[\frac{\alpha H\sqrt{t}}{T_o\sqrt{k\rho c}} \times F(\beta\sqrt{at}) \;,\; \frac{E}{RT_o}\right] \\ \frac{\Delta W}{\rho A\sqrt{at}} &= G_1\left[\frac{\alpha H\sqrt{t}}{T_o\sqrt{k\rho c}} \times F(\beta\sqrt{at}) \;,\; \frac{E}{RT_o}\right] \end{aligned}\right\} \qquad (24)$$

and for rate-controlled charring and weight loss

$$\left.\begin{aligned} \frac{\rho c d T_o}{\alpha Q} &= G_2\left[\mu t \;,\; \frac{E}{RT_o}\right] \\ \frac{\Delta W c T_o}{\alpha A Q} &= G_3\left[\mu t \;,\; \frac{E}{RT_o}\right] \end{aligned}\right\} \qquad (25)$$

Correlation of NRDL Data

Depth of char and weight loss data of the NRDL represent the most extensive data on a single species of wood and are also documented in regard to their statistical reliability. For these reasons the author has selected this set of data as the primary basis of comparison.

The first objective is to delineate between the assumptions of rate- or diffusion-controlled charring. Figures 5 and 6 show the results of applying the proposed depth of char correlation for a rate-controlled process (equation (25)). The reaction velocity constant μ and E/RT_o are constants for this species of wood and as such do not appear on these plots. The absorptivity of the unexposed sample α is also constant and has been assumed unity for reasons which will appear later. Other thermal constants have been computed at zero moisture (dry basis). This does not invalidate the procedure since use of properties evaluated at current moisture (wet basis) would shift all data points by the same amount. Rate-controlled weight loss correlations are not shown since they are characteristically similar to those shown for depth of char.

6/ Subscripts are dropped in the interest of generality. Property values are those of the unexposed sample.

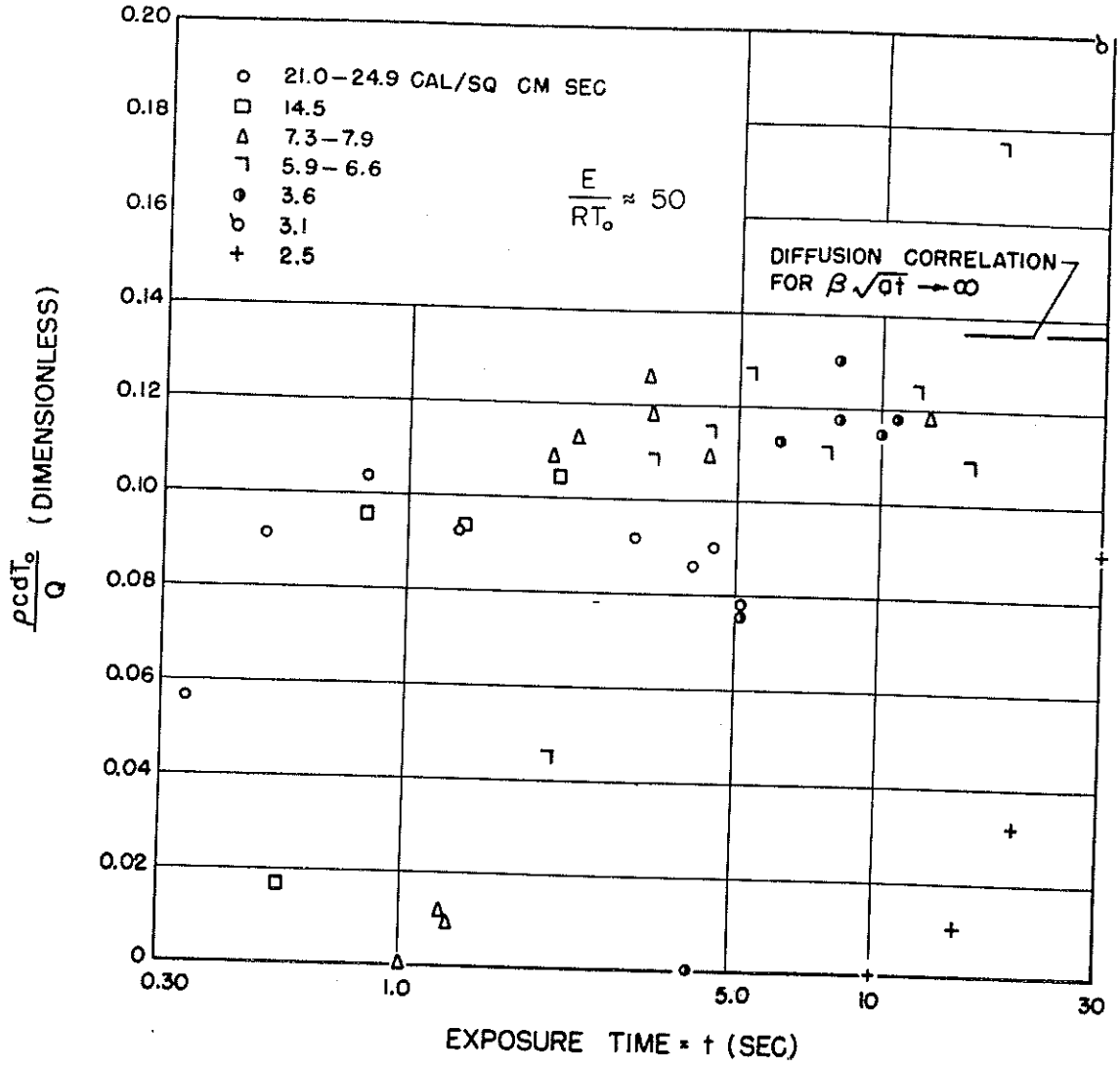

Figure 5.--NRDL square wave depth of char data--rate-controlled basis (T_o = 298°K)

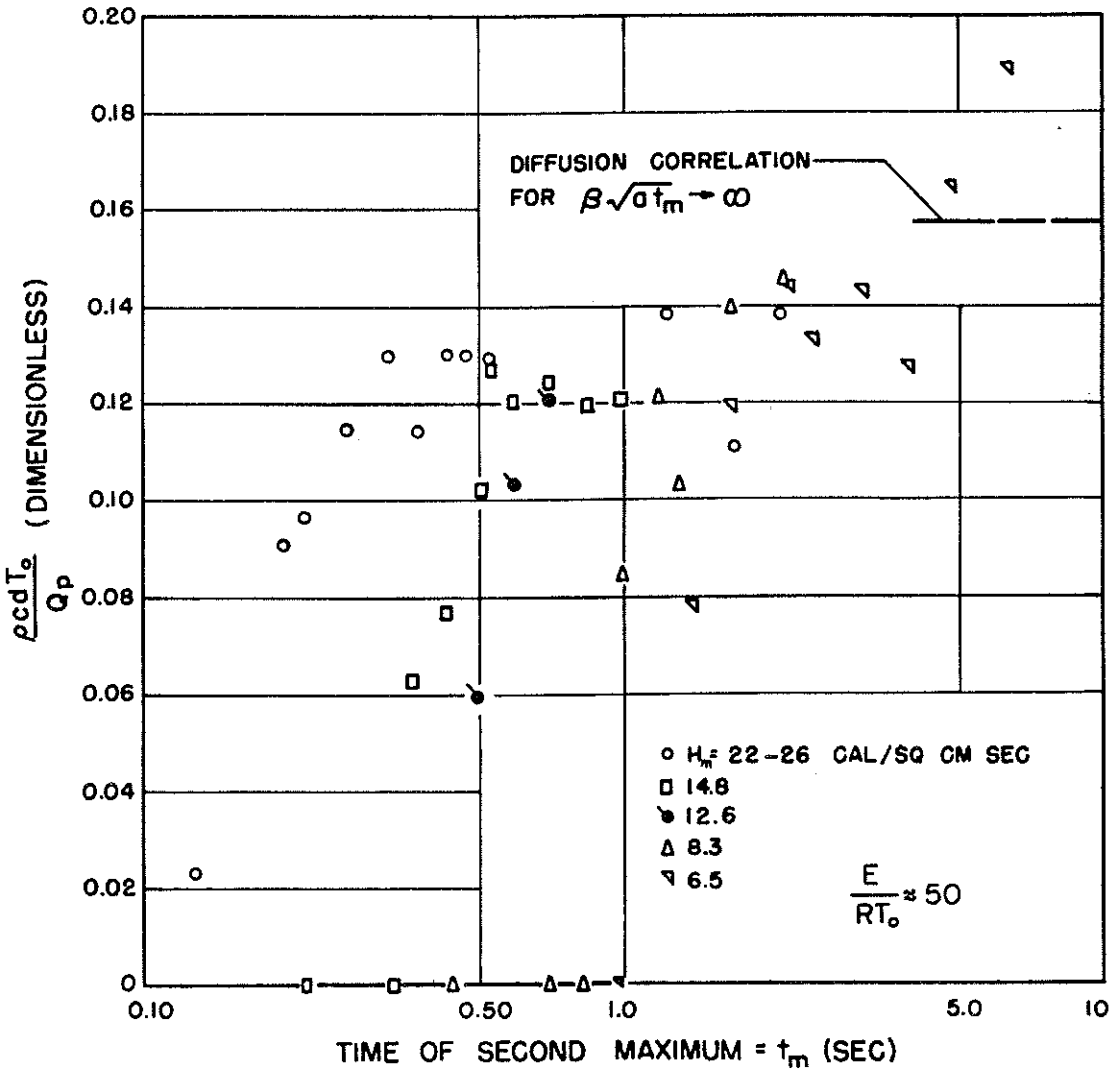

Figure 6.--NRDL field pulse depth of char data--rate-controlled basis (T_o = 298°K)

Depth of char data for the square wave exposure are correlated on a diffusion-controlled basis in figure 7, albeit to a somewhat reduced scale. Data are plotted uncorrected for diathermancy, i.e., $F(\beta\sqrt{at}) = 1$. The greater degree of correlation on the later basis is evident, especially during the initial (transient) stages of charring. Correlation of uncorrected field pulse data (not shown) presents a corresponding degree of correlation. Thus it appears that the more proper procedure is to present charring data in accordance with the correlations suggested by equation (24), i.e., diffusion-controlled basis.

Examination of figure 7 shows that at higher irradiance levels smaller char depths result at the same value of $H\sqrt{t}$ than at lower irradiance levels. This differential decreases as time increases indicating that wood is to some extent diathermanous, even though the surface is charred. When the irradiance modulus is corrected for diathermancy (figure 8) by multiplying by $F(\beta\sqrt{at})$, the correlation is substantially improved. (Note the better correlation of the 21 cal/cm^2 sec data with the 3.6 cal/cm^2 sec data.) The value of absorption coefficient was empirically chosen as $\beta = 100$ cm^{-1} to afford the best fit.[7] Gardon (33,p.20) concludes that for uncharred wood $\beta = 10$ cm^{-1} or greater, which suggests that $\beta = 100$ cm^{-1} is at least the correct order of magnitude for charred wood.

The maximum correction applied amounts to 25 percent, i.e., $F(\beta\sqrt{at}) = 0.75$. In this respect the applied correction may be considered a perturbation and as such the assumption made during derivation of the dimensionless moduli was essentially correct.

Depth of char correlation is displayed in figure 9 with corresponding standard deviations.[8] The solid curve represents the best visual fit through the data, exclusive of the 2.5 cal/cm^2 sec irradiance level. The approach toward the 1:2 slope indicates steady state as previously defined. Apparent deviations from this condition at large values of char depth will be discussed later.

Weight loss data for square wave exposure, corrected for diathermancy, are shown in a similar manner in figures 10 and 11. In this case the 1:1 slope indicates steady state.

7/ This value of absorption coefficient is assumed constant, independent of species.

8/ Ninety-five percent confidence band equals ±2 standard deviations.

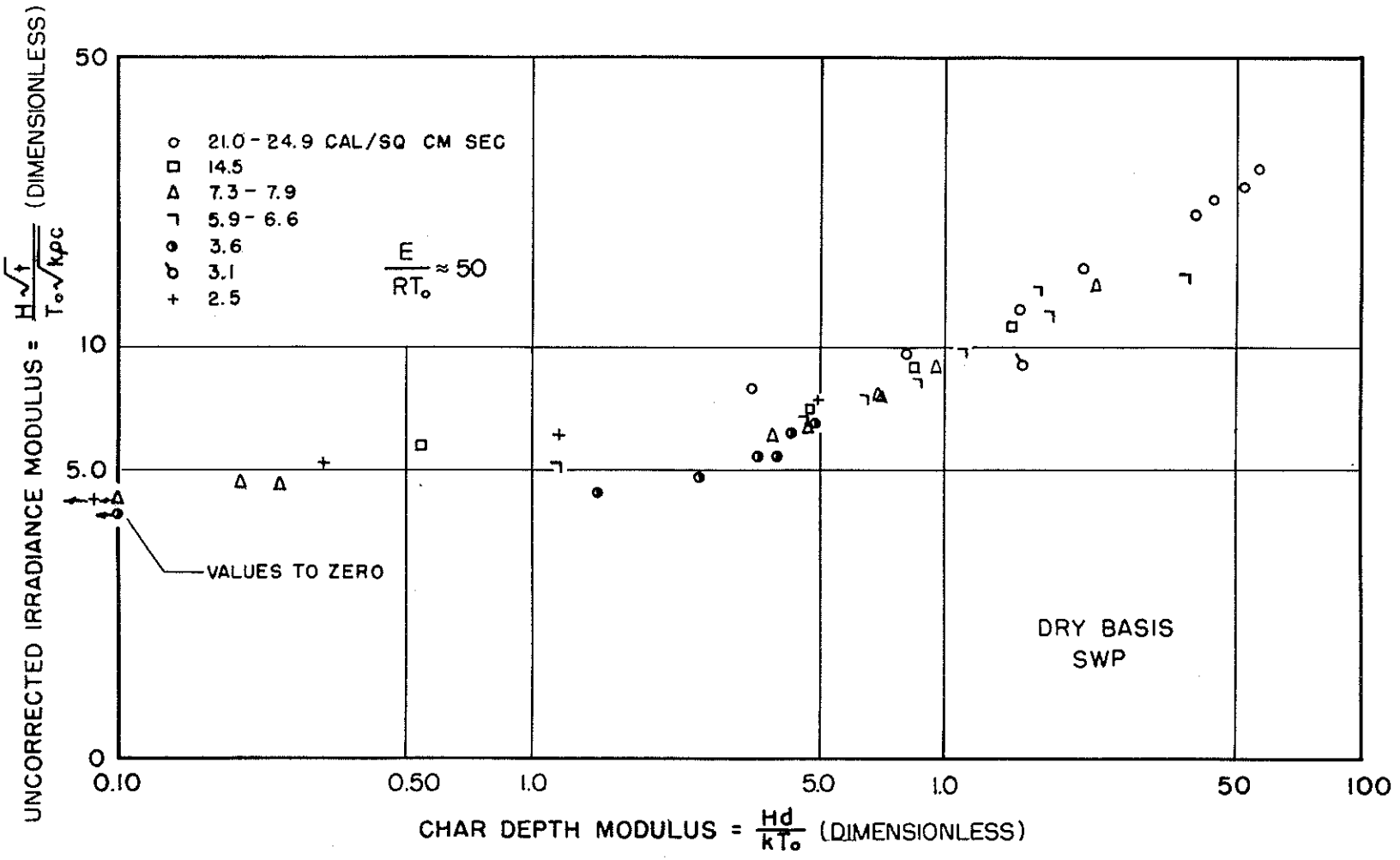

Figure 7.--NRDL square wave depth of char data--diffusion-controlled basis (T_o = 298°K)

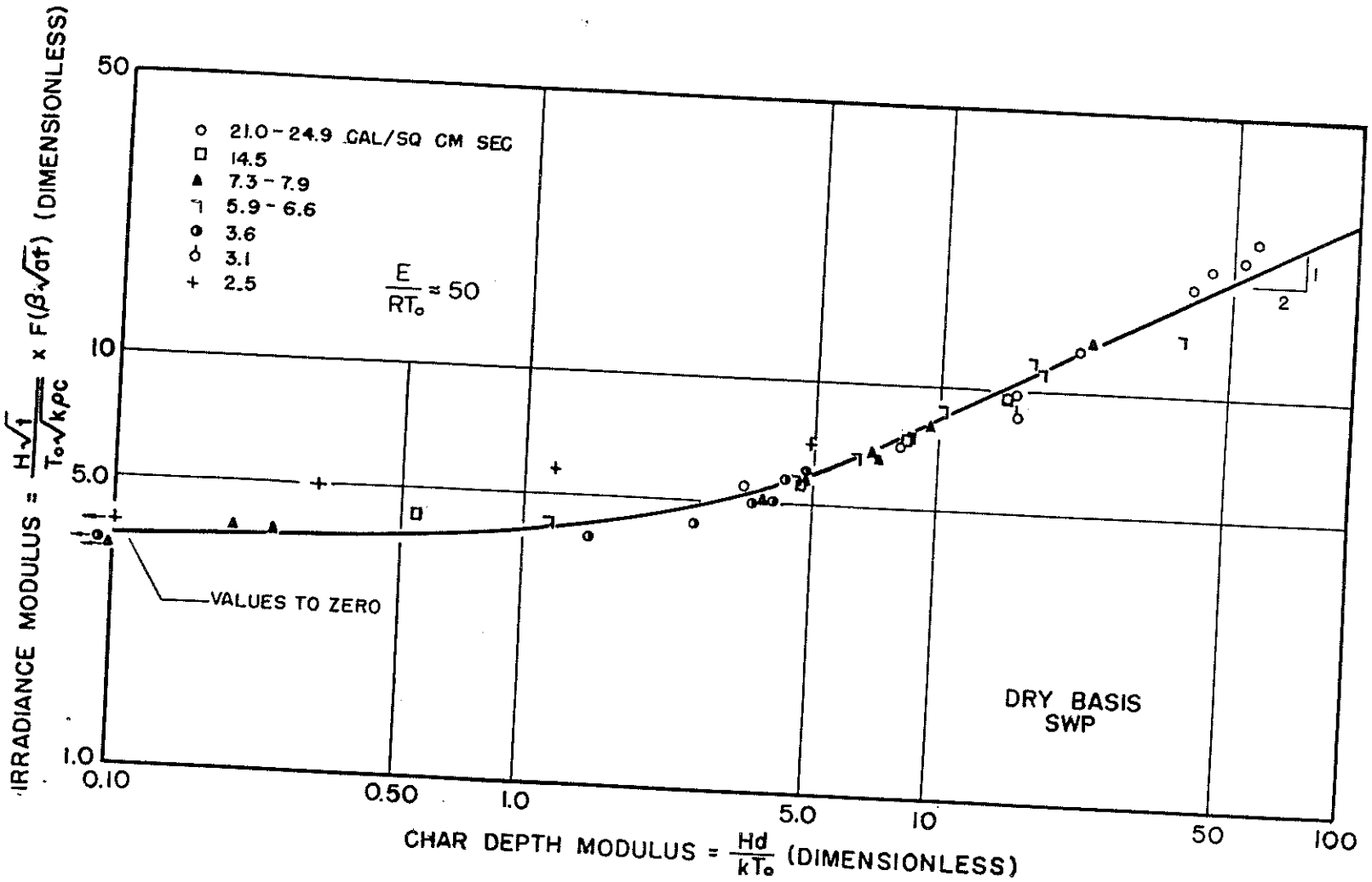

Figure 8.--NRDL square wave depth of char data (heart willow) corrected for diathermancy (β = 100 cm^{-1}) and showing effect of irradiance level (T_o = 298°K)

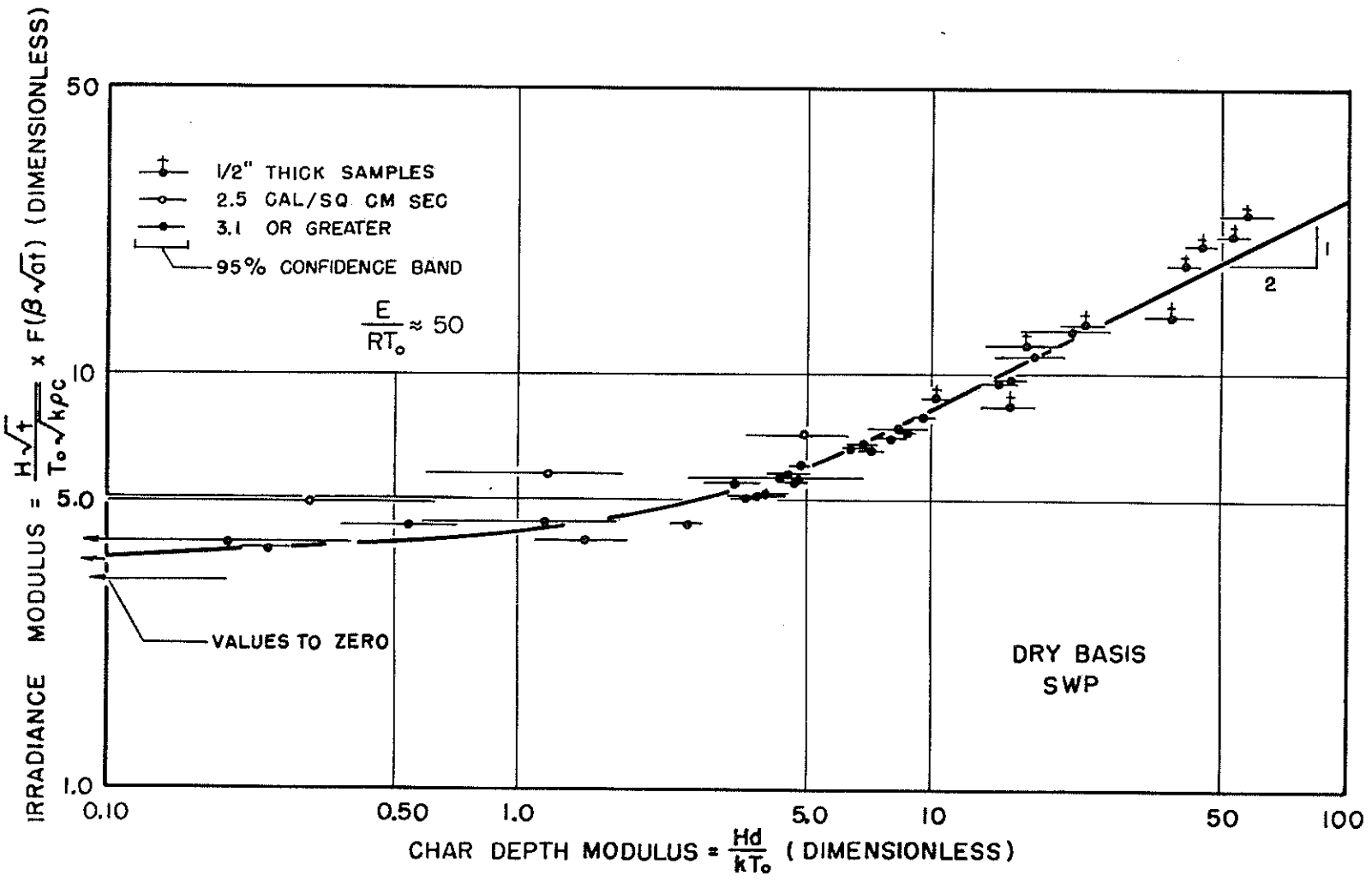

Figure 9.--NRDL square wave depth of char data (heart willow) showing statistical errors in measurement of char depth (β = 100 cm^{-1}, T_o = 298°K)

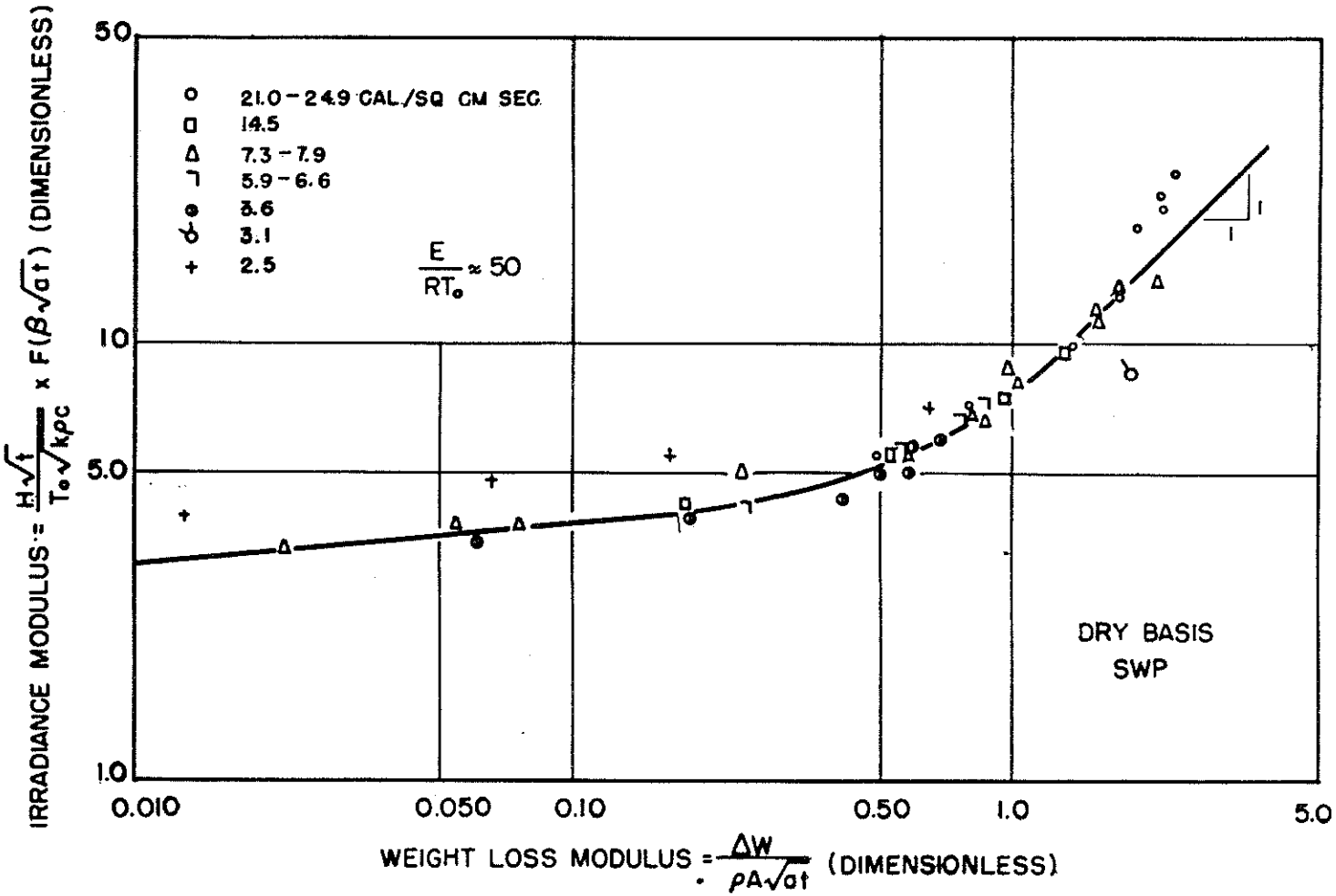

Figure 10.--NRDL square wave weight loss data (heart willow) showing effect of irradiance level (β = 100 cm^{-1}, T_o = 298°K)

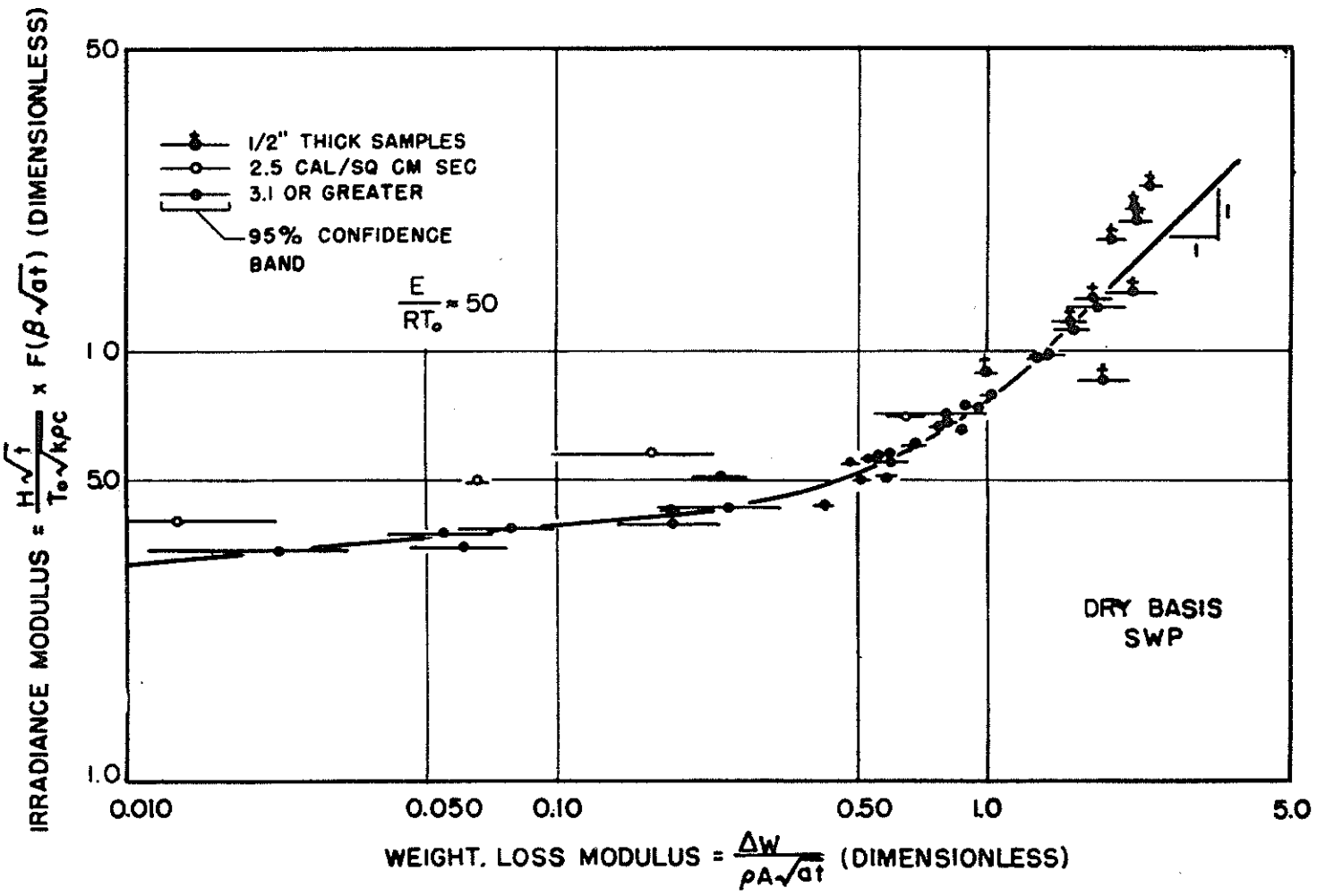

Figure 11.--NRDL square wave weight loss data (heart willow) showing statistical errors in measurement of weight loss (β = 100 cm^{-1}, T_o = 298°K)

Charring data for the simulated field pulse exposures are treated in a corresponding manner in figures 12, 13, 14, and 15. Use of the identical correction for diathermancy, i.e., $F(\beta\sqrt{at_m})$, is of course not rigorously correct. The function F will necessarily be numerically different for the square wave and field pulse exposures; however, the general behavior will be much the same and values are expected to be of the same magnitude. Due to the lack of an analytical solution for the latter case we must apply the square wave correction in the manner indicated more as an order of magnitude than an exact correction. Careful examination of figures 11 and 13 (cf., H_m = 22-26 cal/cm^{2}sec) indeed indicates an over-correction of the irradiance modulus.

The similarity between figures 8 and 12, and figures 10 and 14 is striking although not unexpected. By simultaneous horizontal and vertical translations the field pulse data may be superimposed upon the square wave data. This procedure results in the relationships between the square and field pulse irradiance and times scales

$$\left.\begin{aligned} H &= 0.60\, H_m \\ t &= 4.0\, t_m \end{aligned}\right\} \qquad (26)$$

which define the "equivalent square wave exposure."

Field pulse data are plotted in terms of the equivalent square wave in figures 16 and 17. Comparison with the square wave data is excellent over the entire range considering the standard deviation of the individual points. The weight loss curves appear slightly displaced (10 to 15 percent) since equation (26) was derived primarily from the depth of char correlations.

Attention should be called to those points labeled 12.6 cal/cm^{2}sec in figures 16 and 17.[9/] Data for this irradiance level were determined with a specimen diameter of 3/4-inch (A = 2.90 cm^2) while all others represent a specimen diameter of 3/8-inch (A = 0.745 cm^2). Agreement of the larger diameter specimen data is excellent.

9/ Unpublished data, private communication from C. P. Butler.

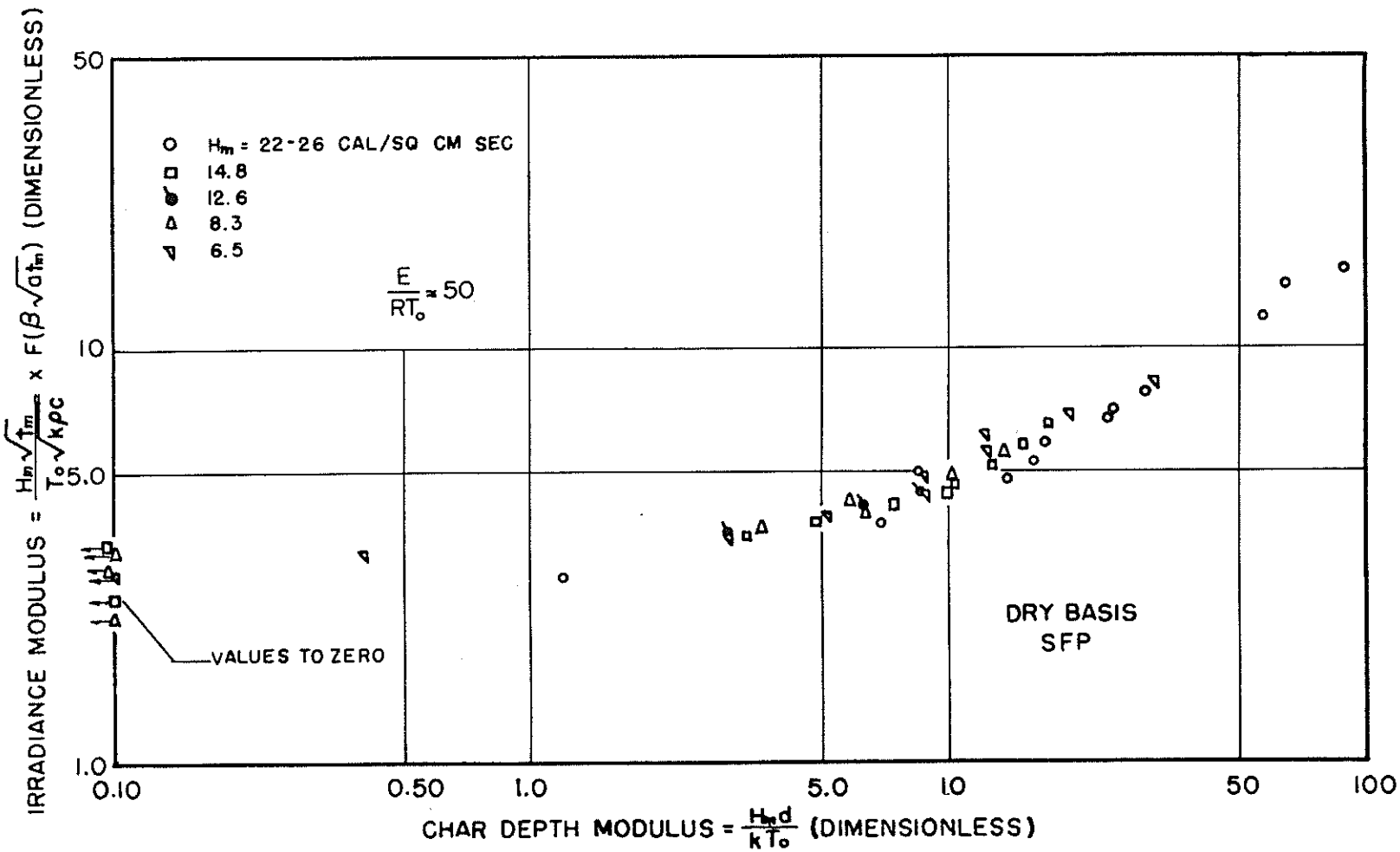

Figure 12.--NRDL field pulse depth of char data (heart willow) showing effect of irradiance level (β = 100 cm^{-1}, T_o = 298°K)

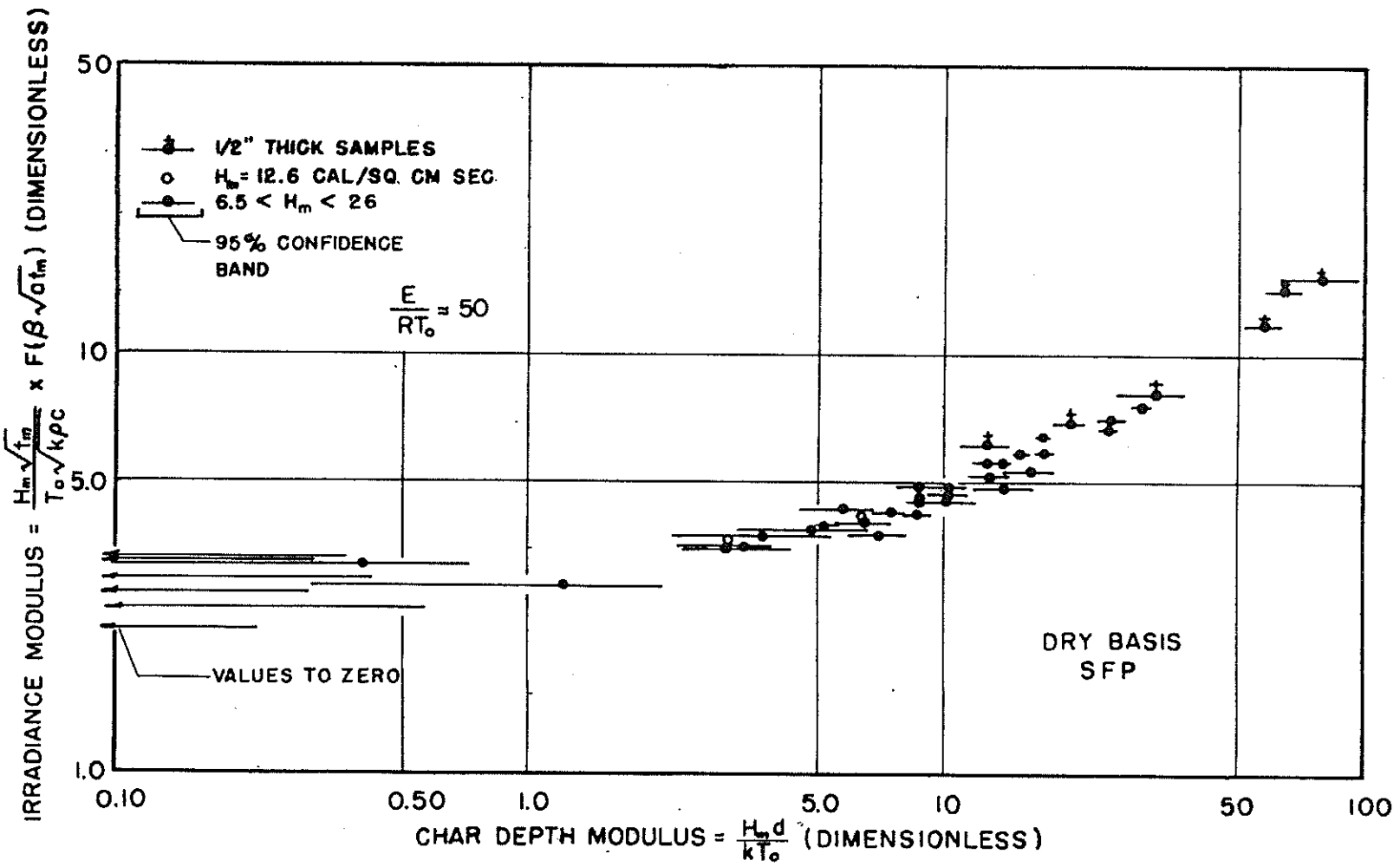

Figure 13.--NRDL field pulse depth of char data (heart willow) showing statistical errors in measurement of char depth (β = 100 cm^{-1}, T_o = 298°K)

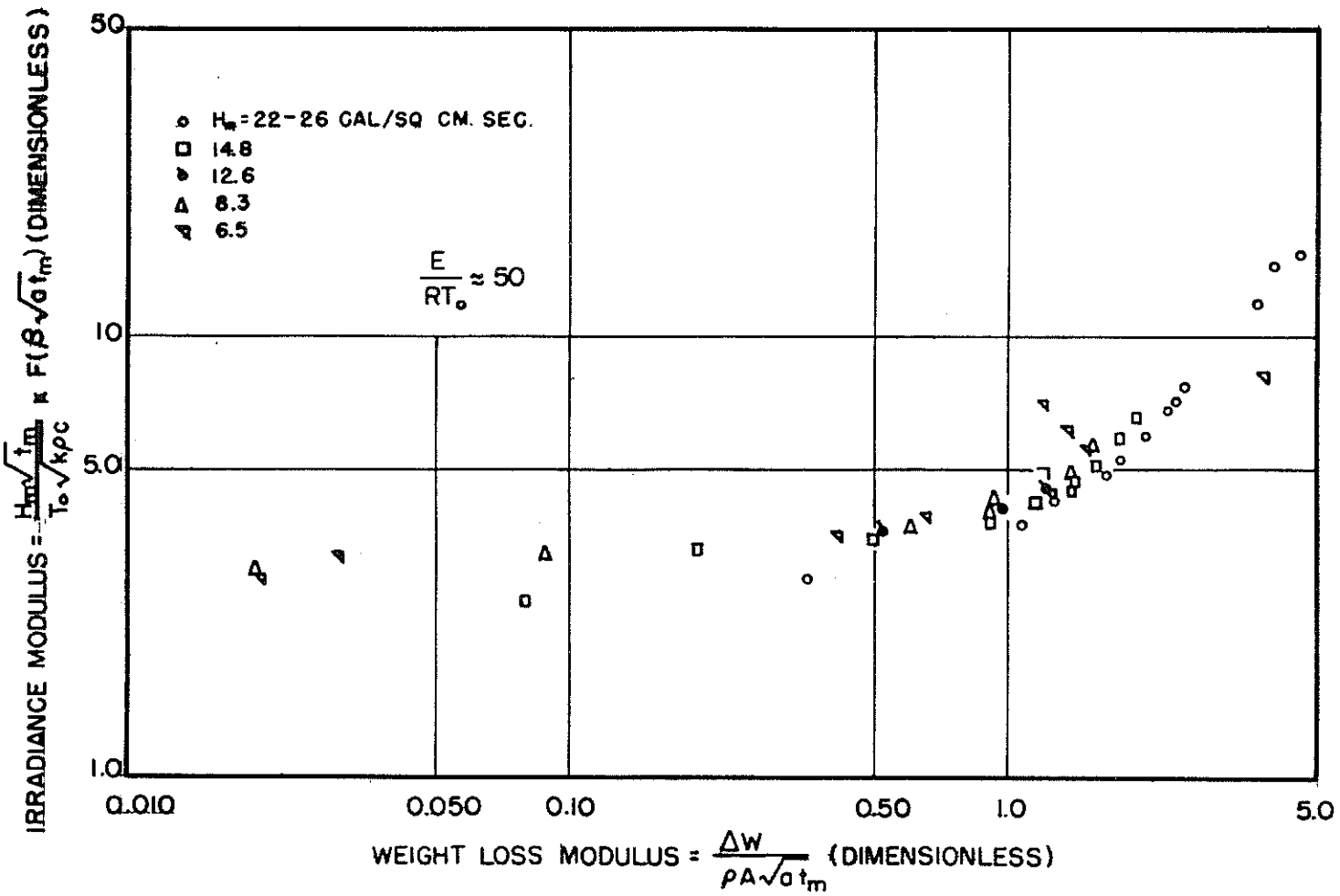

Figure 14.--NRDL field pulse weight loss data (heart willow) showing effect of irradiance level (β = 100 cm^{-1}, T_o = 298°K)

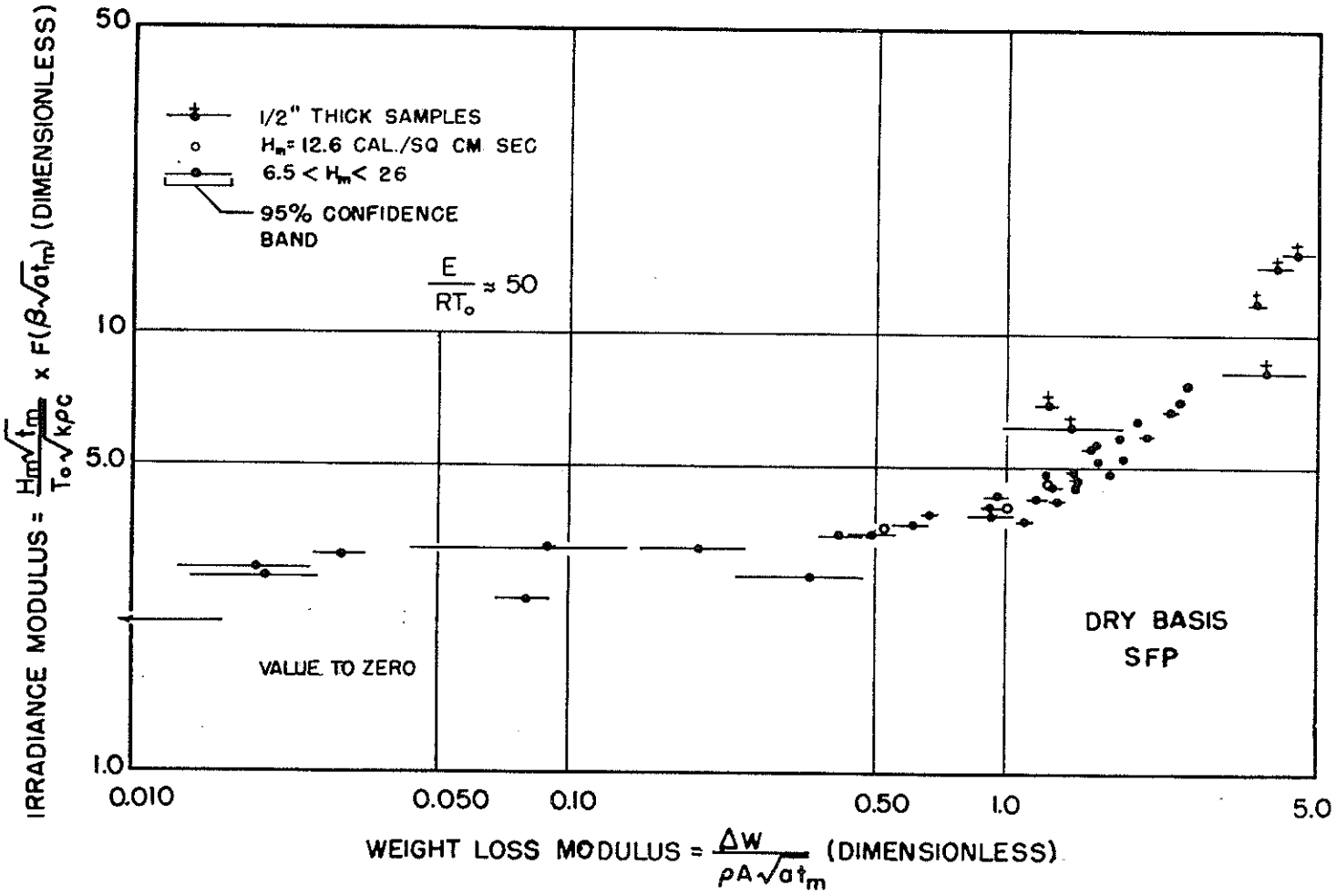

Figure 15.--NRDL field pulse weight loss data (heart willow) showing statistical errors in measurement of weight loss (β = 100 cm^{-1})

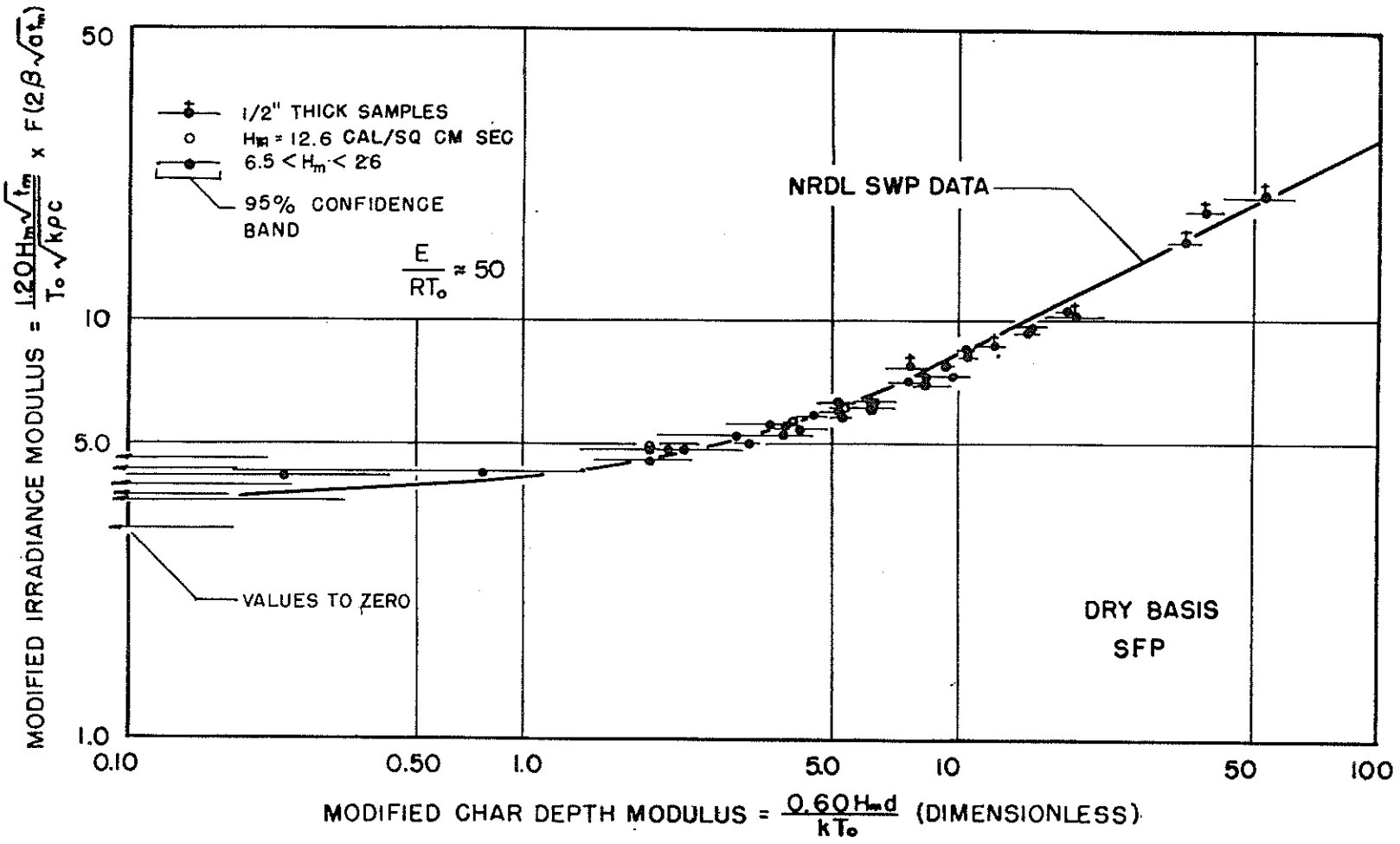

Figure 16.--NRDL field pulse depth of char data (heart willow) based on equivalent square wave pulse (β = 100 cm^{-1}, T_o = 298°K)

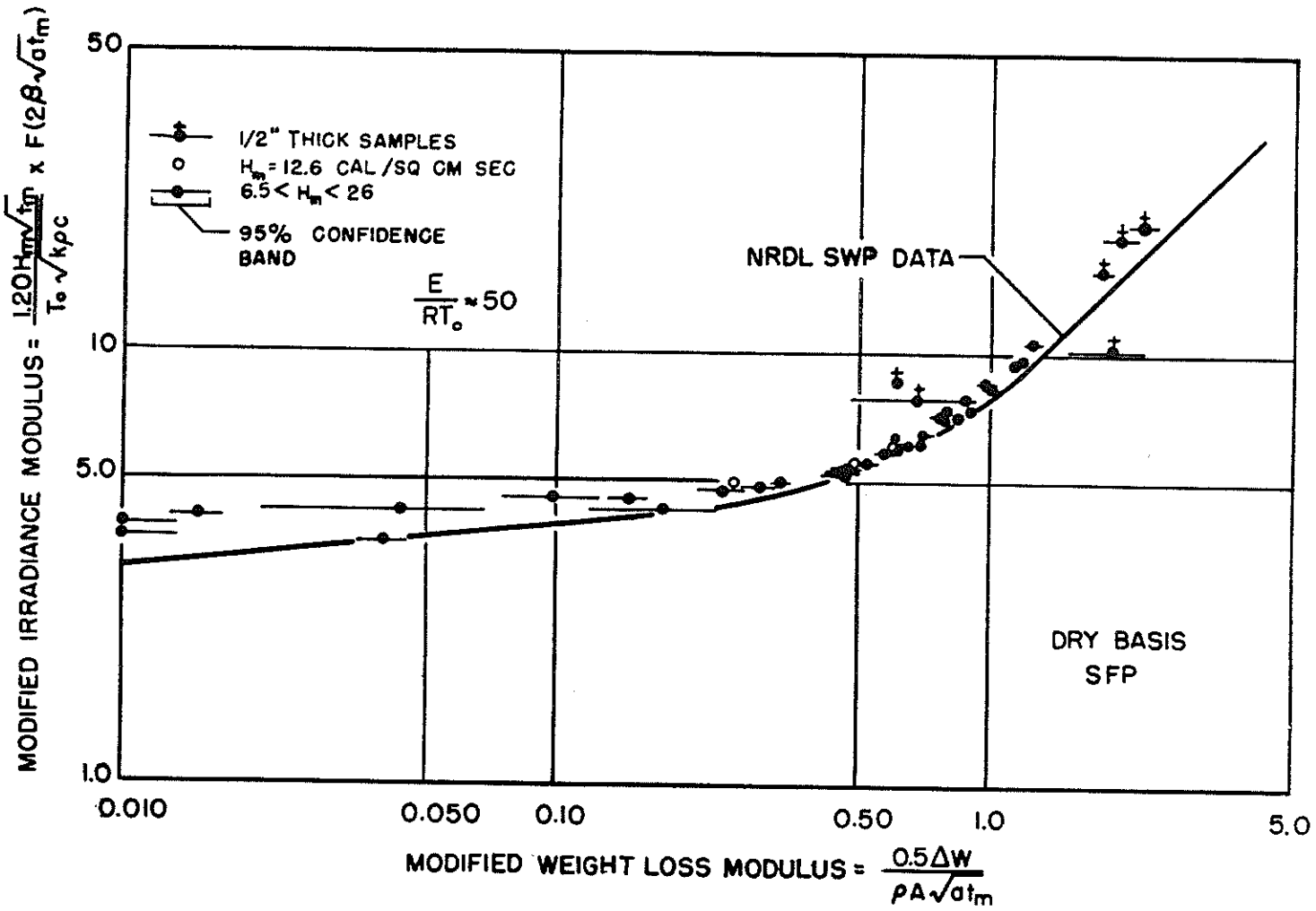

Figure 17.--NRDL field pulse weight loss data (heart willow) based on equivalent square wave pulse (β = 100 cm^{-1}, T_o = 298°K)

Correlation of NBS and MIT Laboratory Data

Laboratory data on depth of char for square wave exposure are correlated on a dimensionless basis in figure 18. NBS data are shown on a dry basis using thermal constants of table 2. MIT exposures were made on ovendry samples so that wet and dry bases coincide. NRDL data and the previously determined correlation are shown for comparison. The NBS and MIT data correlate between species within the maximum spread of data for a single species, about ±25 percent. On the average, the char depth modulus appears 25 percent less than that determined by NRDL.

Since the MIT data represent the only depth of char measurements made on ovendry wood it is interesting to effect a comparison on both wet and dry property bases. Figure 19 displays the NRDL correlation on a dry basis and on a wet basis. Use of wet thermal property values results in a uniform shift of all NRDL data points in a direction away from the MIT data. NBS data correlated on a wet basis would result in a similar shift of approximately the same magnitude. The reason for use of dry properties is now evident; the dry basis affords the better correlation with depth of char measurements on ovendry wood.

NBS weight loss measurements on ovendry wood exposed at an irradiance level of 8.5 cal/cm^{2}sec are compared with the NRDL data correlation in figure 20. Specimen area was 3/4 x 3/4 inch (A = 3.63 cm^2). Agreement with NRDL data on a dry basis is excellent although this result is not conclusive as will be discussed later.

Correlation of NBS Field Data

Depth of char measurements on balsa and mahogany exposed during Operation BUSTER are compared with NRDL simulated field pulse data correlation in figure 21. Thermal energy received at each of the three specimen stations were computed from the shot geometry and thermal energy-distance curves reported in the final thermal radiation measurements report (37). Peak pulse irradiance values were found by dividing energy by the corresponding pulse shape factor and time to second maximum[10/] reported in (38, sheet 1a.1). Since specimen moisture contents are unknown the advantage of being able to use dry properties is apparent.

Correlation of NML Data

Depth of char measurements have been made by NML using both the dynamic (moving strip) and static methods of exposure. Dynamic exposure results are plotted (6) as energy vs depth of char. Exposure times were

---

10/ $H_m = \frac{Q_p}{P\, t_m}$; where $P = \frac{Q_p}{H_m\, t_m}$

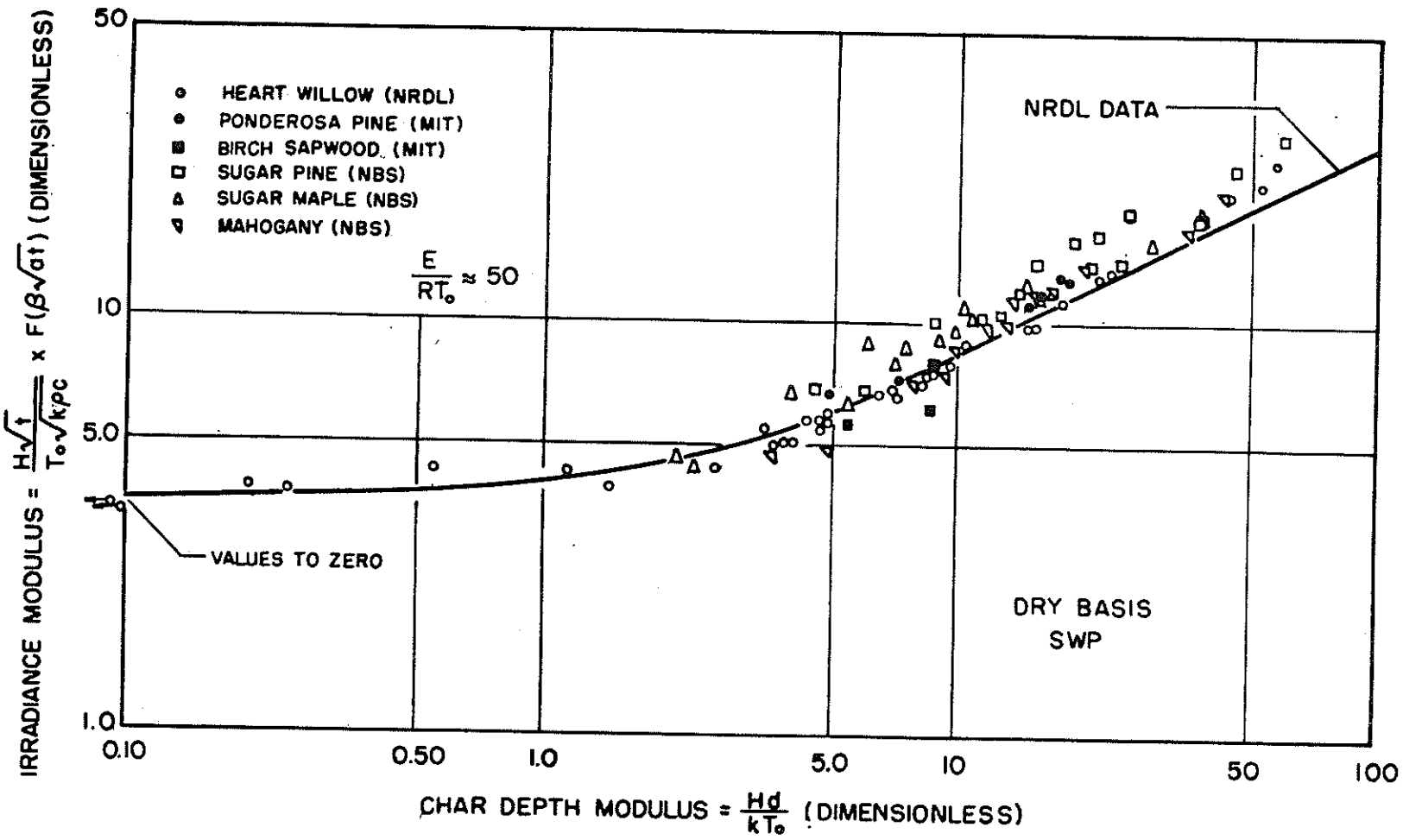

Figure 18.--MIT and NBS square wave depth of char data (β = 100 cm^{-1}, $298 \leq T_o \leq 313^oK$)

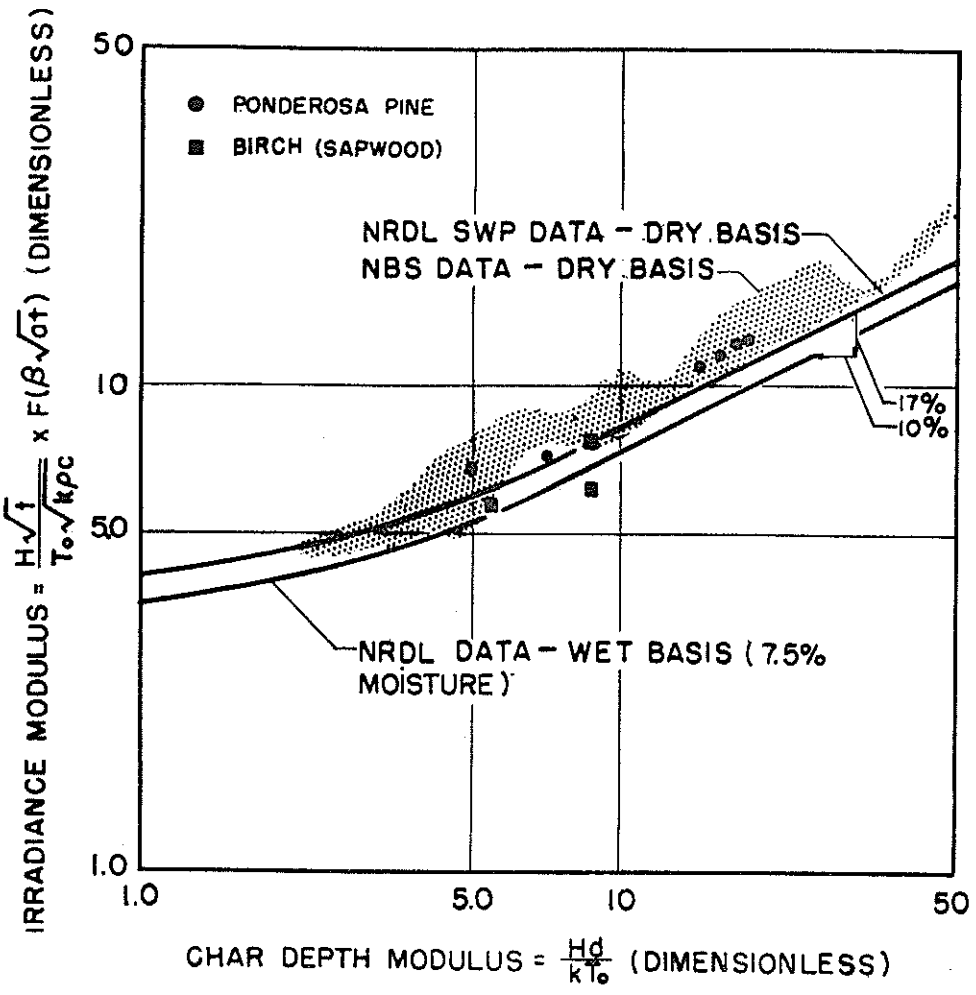

Figure 19--Comparison of wet and dry basis for depth of char correlation

Correlation of NML Data

Depth of char measurements have been made by NML using both the dynamic (moving strip) and static methods of exposure. Dynamic exposure results are plotted (6) as energy vs depth of char. Exposure times were derived by dividing energy values read from the presented curves by the irradiance, 85 cal/cm^2 sec. These results are compared with the NRDL data correlation in figure 22.

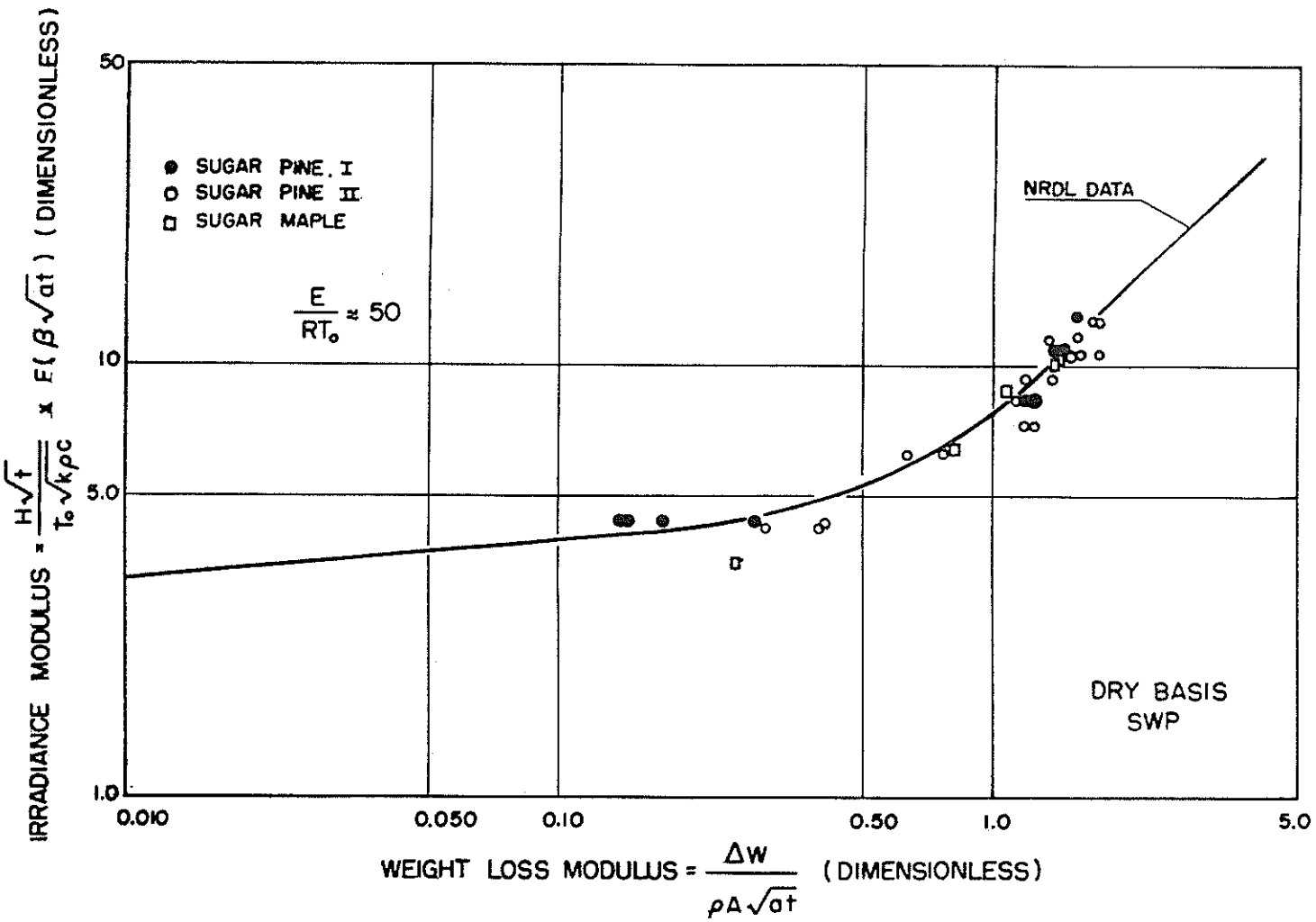

Figure 20.--NBS square wave weight loss data, A = 3.63 cm^2 (β = 100 cm^{-1}, T_o = 298°K)

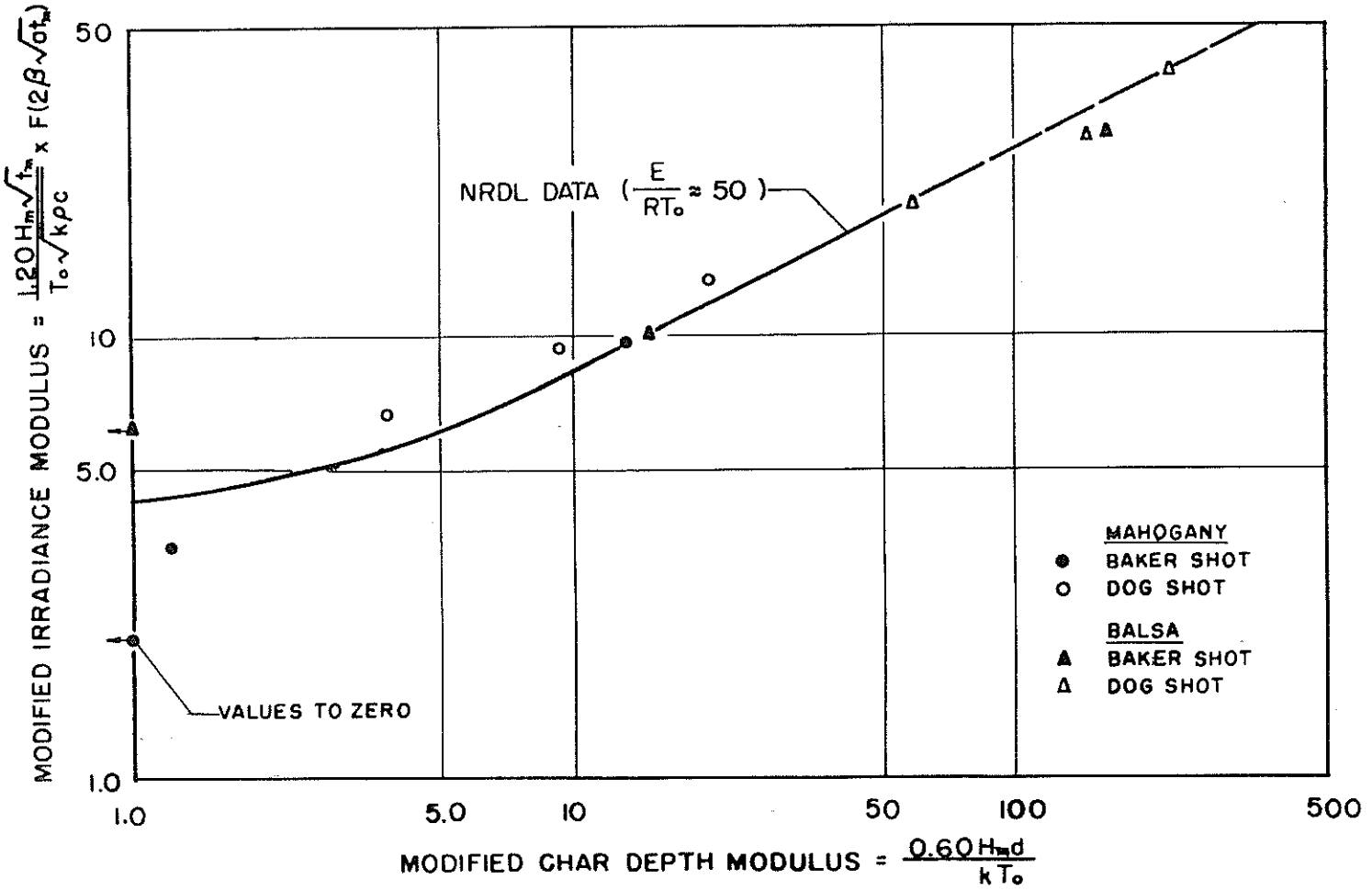

Figure 21.--NBS depth of char data, Operation BUSTER (β = 100 cm^{-1}, T_o = 285°K)

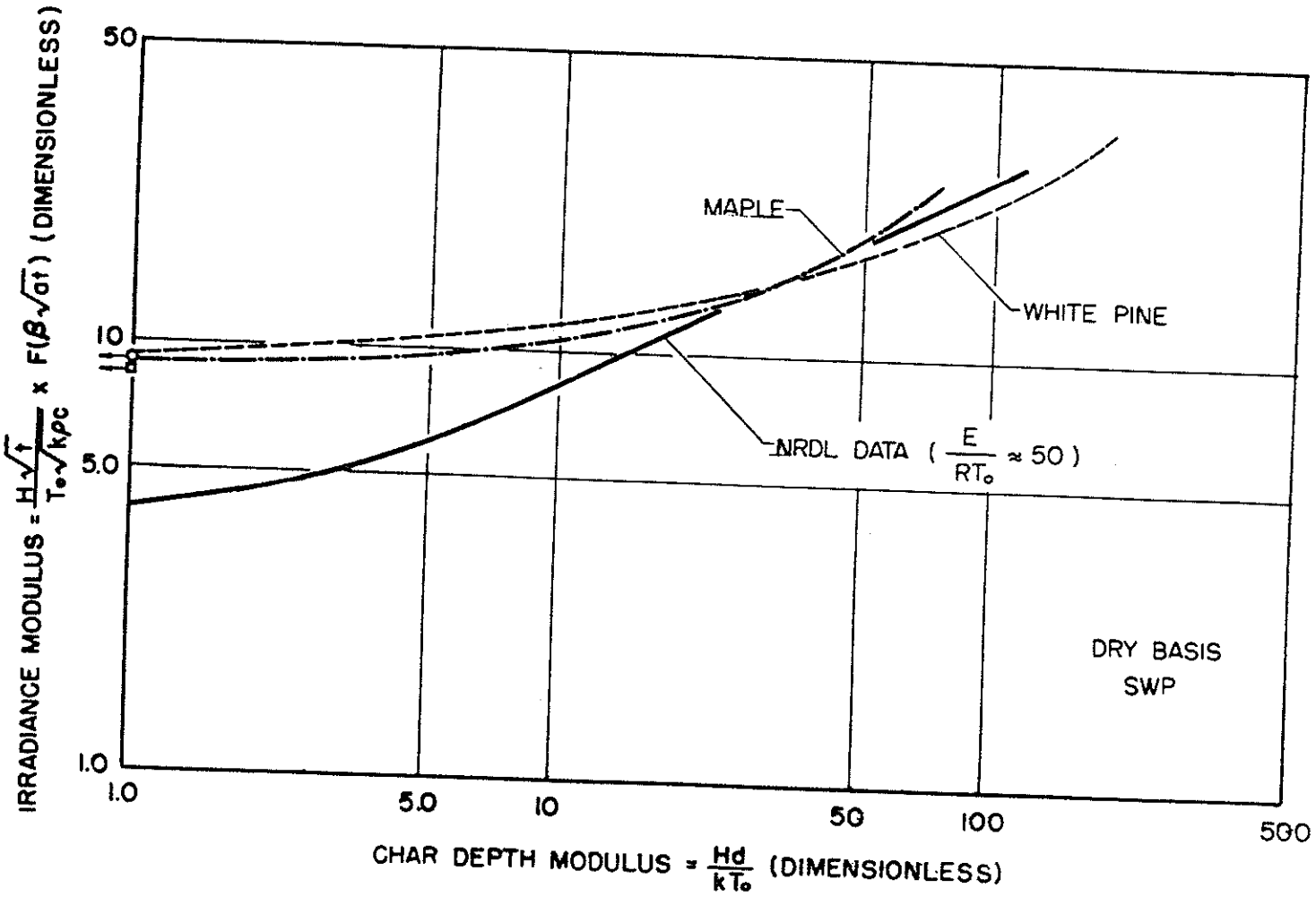

Figure 22.--NML dynamic exposure depth of char data, H = 85 cal/cm^{2}sec (β = 100 cm^{-1}, T_o = 298°K)

derived by dividing energy values read from the presented curves by the irradiance, 85 cal/cm^{2}sec. These results are compared with the NRDL data correlation in figure 22.

Static exposure results are presented (5) as energy vs irradiance for incremental values of char depth, i.e., 0.2, 0.3 ..... 1.8 mm. Threshold,[11] blackening,[11] and burn-through (3.2 mm) values are also presented. Exposure times were derived by dividing energy values corresponding to plotted points by the corresponding irradiance. These points are presented for integral values of char depth and as such reflect any "smoothing" of data during this procedure. Figure 23 displays the dimensionless plotting of these results.

Irradiance modulus corresponding to threshold damage and surface blackening are plotted vs irradiance in figure 24 for $\beta = 100$ cm^{-1} and for $\beta = 10$ cm^{-1}. Use of the latter value greatly improves the correlation, since the irradiance modulus for threshold effects should be independent of irradiance level.

DISCUSSION

When considered by themselves the NRDL data appear correlated within the confidence level associated with determination of the plotted points (±15 percent for depth of char, ±10 percent for weight loss), excepting the 2.5 cal/cm^{2}sec square wave exposures (figure 9). For this irradiance level the irradiance modulus is substantially greater at corresponding values of both char depth and weight loss moduli than indicated by their respective correlations. Back radiation heat losses are, nondimensionally, a function of $(1 - \frac{\epsilon \sigma T_m^4}{\alpha H})$, where $0 < \frac{\epsilon \sigma T_m^4}{\alpha H} \leqslant 1$. The greater the ratio, the greater the relative losses. Since the entire charring process apparently takes place in a temperature range of 200 to 350°C (cf., figure 3), a qualitative estimate of minimum back radiation losses for $H = 2.5$ amounts to 5 or 10 percent. Thus it appears that the greater values of irradiance modulus may be ascribed to surface heat losses. At larger values of irradiance modulus the 2.5 irradiance data tend toward the steady state portion of the correlation curve since steady state is the result of equilibrium existing between net energy supplies and energy required to degrade the wood structure.

---

[11] "Threshold" apparently corresponds to scorching of one grain (summer wood) and "blackening" to scorching of both grains (Banet, L., and Grinoch, P., Critical energies of materials employed in Material Laboratory GREENHOUSE studies. NML Lab. Project 5046-3, Part I final report. 1951.)

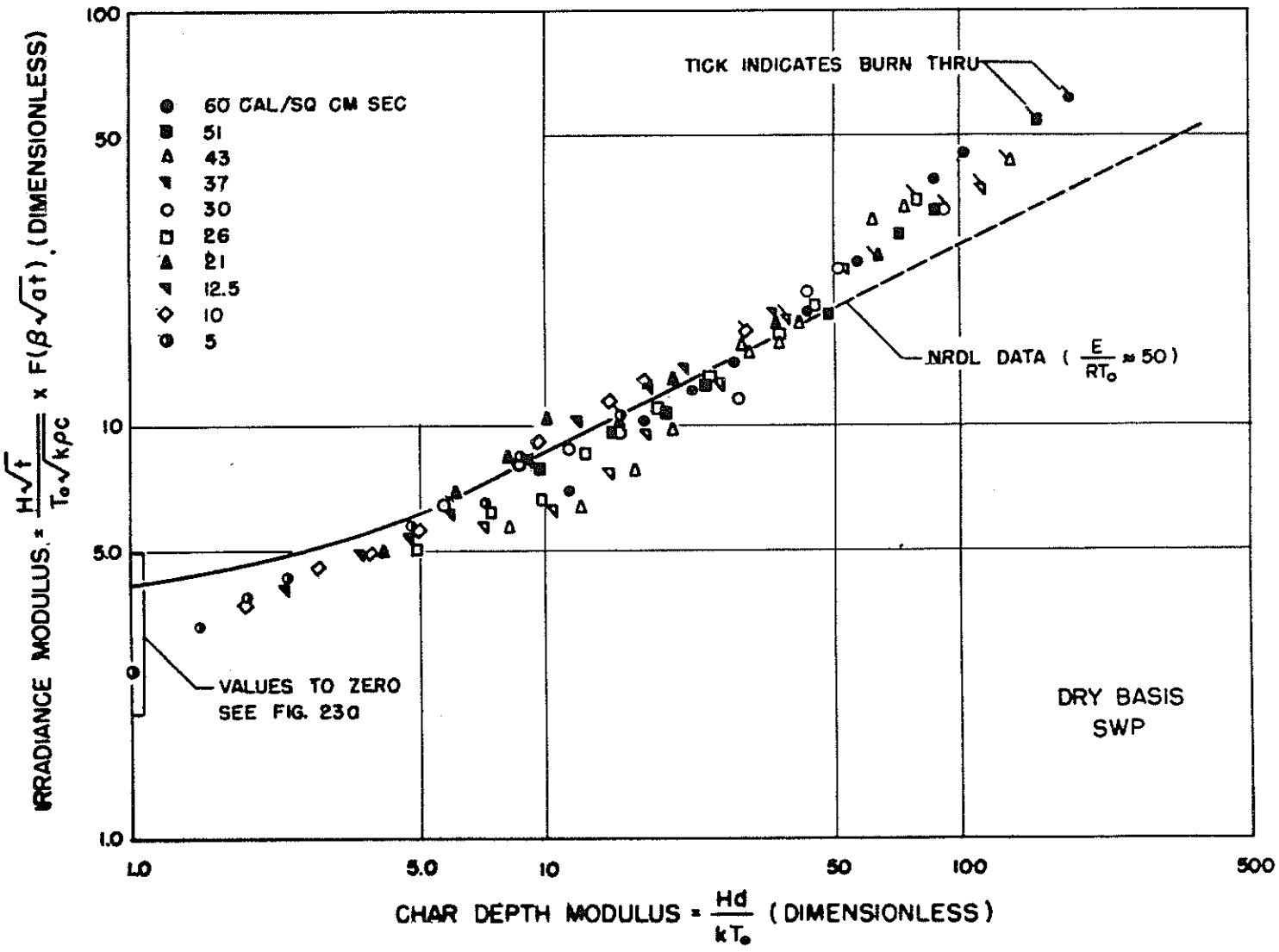

Figure 23.--NML static exposure depth of char data (β = 100 cm^{-1}, T_o = 298°K)

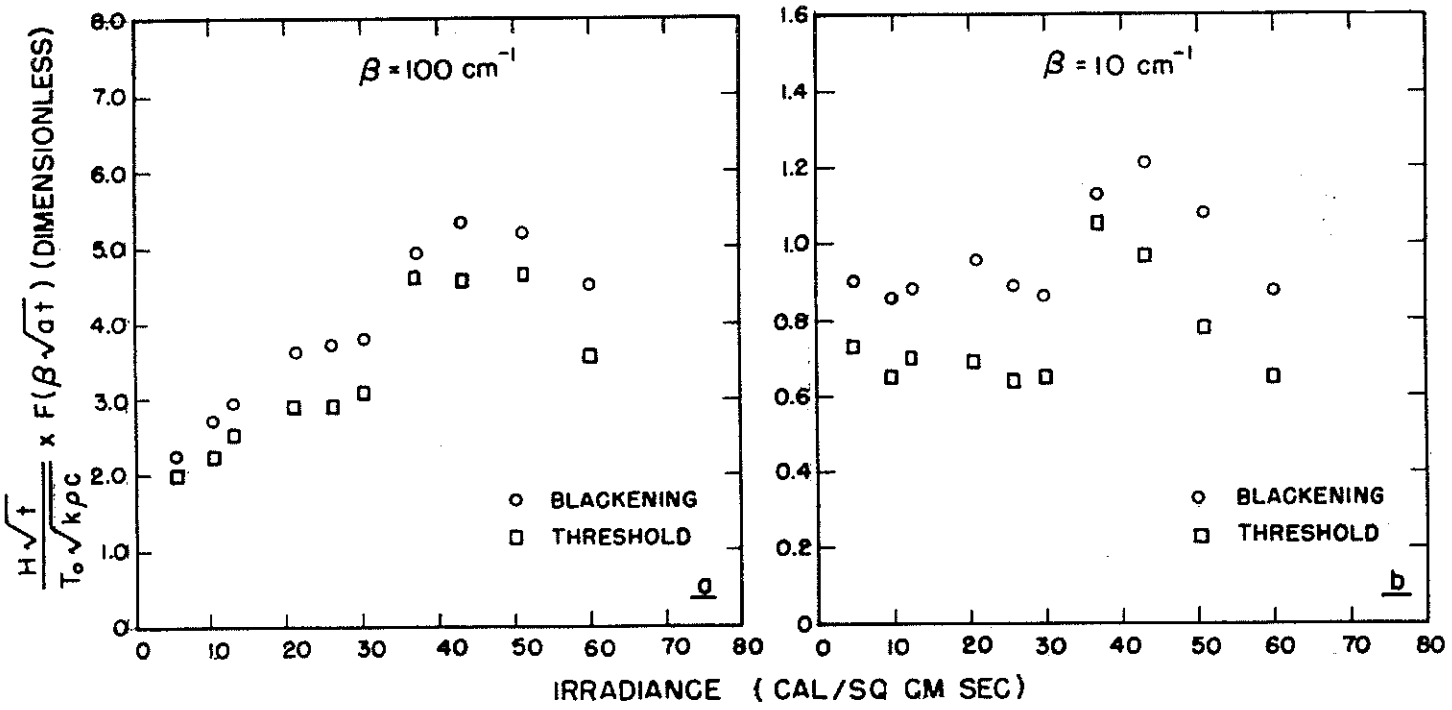

Figure 24.--NML threshold damage data, static exposure

For values of irradiance modulus greater than 20 the tangent of the square wave correlation curve appears to increase, indicating the time rate of charring is decreasing. An apparent increase in slope also appears in the square wave weight loss correlation (figure 11) and in the NML depth of char data (figure 23). This phenomenon, however, does not appear to any great extent in the field pulse data (figures 16 and 17) or in the NBS field data correlation (figure 21). It is for this reason that the author has held the proposed correlation at the 1:2 slope.

It is quite important to speculate on the reason for the divergence of the NRDL data from its proposed course since the slope of the correlation curve measures the time dependence and hence scaling for weapon yield. The NRDL investigators (31,p.25) note that surface spalling results during square wave exposures of the same energy as field pulse exposures wherein spalling does not occur. It is difficult to ascertain the effect of spalling although quite possibly the vapor pockets formed may impede the inward progress of the charred surface.

When char depths become large, surfaces do not remain parallel to their original plane (9,p.13), and the angle of divergence at times exceeds 20 degrees. Aside from causing some difficulty in measurement of char depth the original assumption, that the radiant flux is normal to the surface, is invalidated.

Again at large char depths the surface exothermic process (glowing) proceeds after termination of the exposure (9,p.6). The hypothesis of steady state includes this post-exposure period since it undoubtedly occurs during all exposures, relative, however, to the exposure time. Concurrently it is noted that the back surface temperature did rise considerably when char depths (and weight loss) were large, violating the condition of the semi-infinite solid. Returning to the NML data (figure 23) we note that the "burn through" points correlate well with the remainder of the data. This indicates to the author that the decrease in charring rate is associated with approaching burn-through, i.e., violation of the semi-infinite solid. Furthermore, ratio of maximum char depth to specimen thickness (table 2) is substantially less for the field data, which follow the steady state hypothesis, than for the remaining data.

The question now arises as to the effect on the temperature gradient as the finite solid condition is approached. If one considers only molecular heat losses (conduction) from the rear surface the departure from the semi-infinite solid is expressed in terms of the ratio $\sqrt{k_2\rho_2 c_2} \div \sqrt{k_1\rho_1 c_1}$ where the subscript "1" refers to the finite

solid and "2" to the backing material (39). For air backing up wood this ratio is approximately 50 hence finite solid temperatures would be expected to be greater than those for the semi-infinite solid provided $L/\sqrt{at} > 2$ and $x/L < 0.4$.[12]

When the heat losses from the rear surface are due to convection and radiation, the parameter involved may be written as $h\sqrt{t}/\sqrt{k_1\rho_1 c_1}$ where h includes both the convective and radiation losses. Schack (40,p.37) presents an analysis which results in the value of the heat transfer coefficient just sufficient to maintain the same temperature gradient in the finite solid as the infinite solid. These results (figure 25) are however limited in application since they pertain only to losses during the radiant exposure and do not account for losses during the relaxation of the temperature profile. Furthermore, they do not result in a quantitative estimate of the temperature differential between the two cases. Figure 25 is presented only to demonstrate that as $L/\sqrt{at}$ decreases and time increases the effect of convective losses becomes increasingly important.

Masters' solution (10) for maximum temperatures attained in finite slabs for the boundary condition that the rear surface is insulated ($h = 0$) is useful in estimation of the specimen thickness required to maintain semi-infinite slab conditions. In figure 3 it is demonstrated that the entire charring process probably takes place between 200 to 350°C. It is a necessary condition that finite and semi-infinite slab temperature gradients be identical in this region, i.e.,

$$\frac{\Delta T}{\Delta T_s} \simeq \frac{200-20}{350-20} = 0.55$$

From (10,sheet 4c.4) $L/\sqrt{at} > 4$ satisfies the condition that the rear boundary condition does not influence the temperature gradient above a temperature ratio of 0.5.

Assuming the finite slab thickness, L , to equal the original specimen thickness (table 2) minus the depth of char,[13] values of $L/\sqrt{at}$ were computed for a sampling of NRDL data. Values for all data

---

12/ Cf., (10,Part III,p.6). The same argument as presented therein pertains to the influence of any boundary condition imposed at the rear surface of the finite solid, i.e., at $x = L$.

13/ This condition is rather stringent since there is usually a layer of uncombusted carbon of some thickness above this depth.

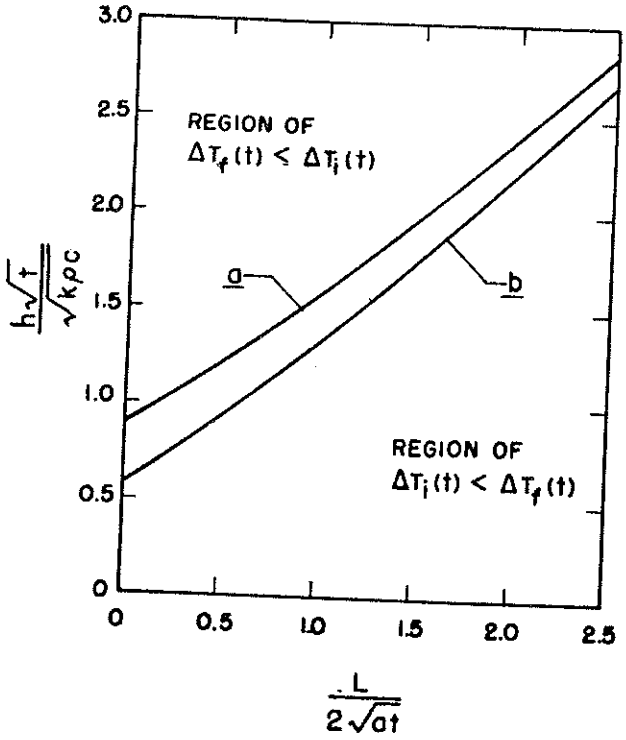

Figure 25--Effect of convective losses at rear surface of a finite solid (after Schack). ΔT (t) designates temperature gradient in finite solid. ΔT (t) designates temperature gradient in semi-infinite solid. Curve a, constant irradiance; curve b, constant surface temperature. (N.B., for illustrative purposes only.)

exceeded 4 excepting the 2.5 irradiance data. Values for the four points originally in question exceeded 12. Thus the hypothesis of the influence of the rear boundary on char depth is seriously in doubt, at least in the light of the very crude estimates allowable in the absence of more elegant theoretical analysis.

The solution to this dilemma is at present experimental, especially since the NML data were obtained under different experimental conditions, i.e., by exposure of a small spot in a relatively large surface. Since this procedure produces a crater, heat flow at the greater char depths may not remain unidirectional, resulting in smaller depths of char compared to the ideal case. Conditions of this type are difficult, however, to evaluate in a quantitative manner.

Along these lines attention should be directed to the NRDL 12.6 cal/cm^{2}sec field pulse exposures (figures 16 and 17), the exposure area for this irradiance level (2.90 cm^2) being four times that of the remainder (0.745 cm^2). Although only three exposure times are reported, the excellent agreement of both depth of char and weight loss data indicates the smaller area was sufficiently large to maintain unidirectional heat flow. It should be noted that these are the only data, known to the author, demonstrating this necessary condition.

Dimensionless correlation of NRDL, MIT, and NBS depth of char data appears to be in satisfactory agreement considering the various techniques used to measure these quantities. The fact that NRDL char depths are approximately 25 percent greater than other investigators may be attributed to the different methods used to measure char depth although this hypothesis is not at all conclusive.

At this point it is well to consider the role of initial temperature, T_o, on the rate of charring and weight loss. When charring proceeds at a steady rate, one observes the apparently anomalous result that for constant char depth or weight loss the energy, Q, increases proportionally to the initial temperature, T_o, (cf., equations (29) and (31), p. 62). One must remember, however, that the presented correlations represent only one of a family of curves of constant parameter E/ERT_o so that as T_o (or E) changes one must move to another curve as indicated by equation (24). Since charring will proceed at an observable rate, unaided by thermal radiation, when the initial temperature approaches 500°K (cf., figure 3), curves of constant E/RT_o must be related such that Q decreases as T_o increases (or E decreases).

The presented data do not clarify the role of T_o (or E/RT_o) since the variation in absolute initial temperature was only about 5 percent. Furthermore specific information is lacking concerning the activation energies for the woods exposed. However, table 1 indicates that for most of these woods, with the possible exception of balsa, E may be taken as 30 kcal/mole within an error of ±10 percent so that E/RT_o equals 50 ±10 percent for the correlations presented. For the present, variations in energy (or irradiance and time) due to initial temperature cannot be predicted to greater accuracy than the accuracy assigned the parameter E/RT_o, i.e., ±10 percent. Consequently variations in initial temperature of this same order cannot be considered as s[illegible] within the accuracy of the proposed correlations.

This result may also be derived in a slightly different manner. Consider an alternate form of equation (24) derived by dividing the irradiance and char depth modulii by E/RT_o.

$$\left.\begin{aligned} \frac{\alpha HRD}{kE} &= G_4 \left[\frac{\alpha HR\sqrt{t}}{E\sqrt{kpc}} \times F\left(\beta\sqrt{at}\right), \frac{E}{RT_o} \right] \\ \frac{\Delta W}{\rho A\sqrt{at}} &= G_5 \left[\frac{\alpha HR\sqrt{t}}{E\sqrt{kpc}} \times F\left(\beta\sqrt{at}\right), \frac{E}{RT_o} \right] \end{aligned}\right\} \qquad (24a)$$

In this form it is readily apparent that the correlations are dependent on knowledge of the activation energy E and that the effect of variation in T_o is the same as that of variations in E.

Hence it is suggested that where the initial temperature varies within the limits, $300^oK \pm 10$ percent ($0 \leqslant T_o \leqslant 60^oC$) then $T_o = 300^oK$ should be used in calculating of correlation parameters. This procedure results in overestimation of char depth and weight loss when the initial temperature is less than 300^oK and underestimation when the temperature is more than 300^oK. This procedure is consistent with the accuracy of the assumption of constant E as discussed above.

Char depth measurements made by NRDL in conjunction with field exposures during Operation TEAPOT (unpublished) have been correlated by the author and lead to char depths 30 percent less than expected from the proposed correlation. These exposures were made on Guatemalan cedar ($\rho_D = 0.47$). Specimens were cut, in general, oblique to the grain[14/] whereas the previous specimens (willow) were cut tangential and the radiant exposures made in the radial direction. Subsequent laboratory measurements on Guatemalan cedar correlated closely with the field data thus confirming the 30 percent differential relative to other species exposed by NRDL. In the absence of a value for activation energy for this tropical species it is difficult to determine whether this increased resistance to charring is the result of a larger value for E because of differences in lignin content or to the increased conductivity due to grain orientation. Since steady state conductivities in the radial

---

14/ MIT and NML exposures appear to be made in the tangential direction. The NBS exposure direction was probably tangential: correspondence from NBS dated 3/21/56.

and tangential directions appear to be substantially the same (p. 15) the observed decrease in char depths is probably due to a larger value of the activation energy. These data illustrate the range of uncertainty in using the presented correlations for species of wood for which thermal properties are not well known.

Property values throughout have been based on dry density primarily due to the better degree of correlation between the NRDL and NBS depth of char data and the MIT data (figure 19). Correlation of NBS weight loss data on a dry basis (figure 20) unfortunately is not conclusive since the variation of irradiance across the span of the NBS specimen was approximately the same, percentage-wise, and in the same direction as the correction between the wet and dry basis correlations of the NRDL data.

This result demonstrates an extremely important criterion regarding investigation into the role of moisture, viz., the irradiance variation across the sample area must be substantially smaller than the variations in weight loss expected from moisture. This is also true, to a lesser extent however, during char depth measurements. Weight loss measurements appear more statistically reliable since they average out spatial variations in properties and as such are more suitable for the type of investigation necessary to determine the role of moisture.

The use of dry properties raises the question as to why better correlation should result on this basis. This procedure is strictly empirical; however, there appears to be some theoretical justification. Moisture has the effect of increasing the rate of thermal degradation of wood (16,p.4), i.e., moisture decreases the activation energy for degradation resulting in more rapid changes in density at lower temperature. At the same time moisture increases the thermal conductivity and specific heat, thus causing lower temperatures in the interior of the solid for the same radiant exposure. The possibility exists that these two opposite effects cancel one another, at least in the moisture range investigated ($M < 8$ percent).

Another empirical choice of properties is that of choosing the absorptivity, α, equal to unity or at least a constant for all species. Hence α does not appear in the irradiance modulus. The data presented in figure 18 represents a range of visual surface color from very light (sugar pine) to dark (mahogany). The lighter species show a tendency to char less than the darker species, the differential being within the scatter of data, however. The assumption of constant absorptivity appears reasonable, at least for char depth moduli greater than 4, since surfaces soon lose their original absorption characteristics as charring takes place.

The lesser char depths may also be the result of an absorption coefficient less than the assumed nominal values of 100 cm^{-1} due to the less dense charcoal formed by the less dense species. However, further discussion of this and other effects such as attenuation of the incident radiation by smoke and surface oxidation reactions are not warranted in light of available data.

The presented relationship demonstrates the reason, aside from measurement errors, for the large standard errors associated with small depths of char. For values of char depth modulus less than 2, char depth is extremely dependent on the irradiance modulus, or if the irradiance and exposure time are constant, upon the thermal properties. Small standard deviations in density will then result in much larger standard deviations in char depth. Conversely the irradiance modulus may be determined without serious error, say ±15 percent, from small non-zero depths of char when measurements have rather large standard deviations.

The extreme dependence of char and weight loss moduli on irradiance modulus in the region of char depth modulus less than 2 may be due to the transient nature of the temperature gradients or to extreme changes in absorption coefficient, or both. To illustrate this consider the NML threshold data (figure 24). Zero char depth when defined in terms of threshold damage or blackening of the surface do not correlate on the proposed basis, i.e., $\beta = 100\ cm^{-1}$, as can be seen from figure 24. A satisfactory correlation should yield results independent of irradiance. This type of threshold damage should be distinguished from "zero depth of char" as reported by NRDL in that the latter data represent measurements which vary between zero and some small finite value comparable to the least count of the instrumentation. The former types of threshold damage refer to visual examination of the surface.

It is reasonable to assume that since the major portion of the energy is delivered prior to "blackening" the value of absorption coefficient should correspond to that of the undamaged surface. If one assumes that the lower limit of Gardon's estimate, $\beta = 10\ cm^{-1}$, the irradiance modulus becomes essentially independent of irradiance level (figure 24). In this case $0.12 < \beta \sqrt{at} < 0.55$ approaches the region of extreme diathermancy where the theoretical surface temperature becomes dependent upon total energy received (equations 20 and 23) rather than primarily upon $H\sqrt{t}$. It is apparent that the absorption coefficient must change rapidly during the initial stages of charring.

A qualitative estimate of the surface temperature for surface "blackening"[15] may be made from the results of figure 24 and equation (20)

$$\frac{\Delta T_s}{T_o} \simeq \frac{2}{\sqrt{\pi}} \times 0.9 \quad ; \Delta T_s \simeq 300^{\circ}C$$

Comparison with figure 3 shows that this temperature is compatible with the temperature range in which the rate of thermal degradation increases extremely rapidly. Robertson (4,p.39) also arrives at the conclusion that rapid charring must take place in the range 280-350°C.

The reader should not consider that the above computations present universal constants, either for a "charring temperature" or for the initial value of absorption coefficient (β = 10 cm^{-1}). These figures are presented only as illustrations of the qualitative agreement of the various phases of the presented material.

Discussion of the NML static exposure measurements (figure 23) has been retained until last, due to the lesser degree of correlation of this data. The large scatter of data in the region of char depth modulus equal to 10 is the result of the anomalous "humps" in the original results. Char depths for irradiance levels above 60 $cal/cm^2 sec$ were not presented due to the ambiguous nature of the maximum irradiance used and the method of attenuation (5,p.14,15). The greater than 1:2 slope, as previously discussed, is attributed to the approach toward the finite solid.[16] Since these data on a single species contain greater divergence than other data on at least five species, a re-evaluation of conclusions regarding the charring process (38,sheet 5g.2) appears to be in order.

The NML dynamic exposures (figure 22) display an entirely different behavior than other exposure methods. The dynamic exposure subjects the material to a radiant pulse which is Gaussian with respect to the timewise variation of irradiance (38,sheet 3a.1). Since it has already been demonstrated that pulse shape is an important parameter in damage correlation, this result is not unexpected. Insufficient data, however, do not allow specification of the equivalent square wave pulse.

15/ We choose this criterion rather than "threshold" since the latter damage is scorching of the summer growth, the density of which is lower than the average for that species. Consequently the $\sqrt{k\rho c}$ will be lower than that assumed in the following calculation.

16/ Note that these specimens were 1/8 inch thick compared with the 1/4 inch thickness primarily used by NRDL.

Recommended correlation functions for square wave and field pulse depth of char and weight loss are displayed in figure 26 for exposures where the radiant flux is radial with reference to the grain geometry and the irradiance is greater than 3 cal/cm^{2}sec. Presented correlations are valid only when the specimen behaves as a semi-infinite solid. Property values are those of the unexposed dry wood. Exposures made oblique or in the tangential direction are expected to yield char depths and weight loss 25 percent less than given by figure 26. As previously discussed correlations are only valid for $E/RT_o = 50 \pm 10$ percent. T_o should be taken as equal to 300°K for all values of initial temperature between 0 and 60°C.

For irradiance moduli greater than 7 both weight loss and char depth achieve steady state and the correlation equations become for the square wave

$$\left.\begin{aligned} \frac{\Delta W}{\rho A\sqrt{at}} &= 0.13\,\frac{H\sqrt{t}}{T_o\sqrt{k\rho c}}\,F(\beta\sqrt{at}) \\ \frac{Hd}{kT_o} &= 0.14\left[\frac{H\sqrt{t}}{T_o\sqrt{k\rho c}}\,F(\beta\sqrt{at})\right]^2 \end{aligned}\right\} \qquad (27)$$

and for the field pulse

$$\left.\begin{aligned} \frac{\Delta W}{\rho A\sqrt{at_m}} &= 0.32\,\frac{H\sqrt{t_m}}{T_o\sqrt{k\rho c}}\,F(2\beta\sqrt{at_m}) \\ \frac{Hd}{kT_o} &= 0.33\left[\frac{H\sqrt{t_m}}{T_o\sqrt{k\rho c}}\,F(2\beta\sqrt{at_m})\right]^2 \end{aligned}\right\} \qquad (28)$$

where F is given by equation (21) or figure 4.

Upon combining terms, equations (27) and (28) yield

$$\left.\begin{aligned} \frac{c\Delta WT_o}{AQ} &= 0.13\,F(\beta\sqrt{at}) \\ \frac{\rho cdT_o}{Q} &= 0.14\,F^2(\beta\sqrt{at}) \end{aligned}\right\} \qquad (29)$$

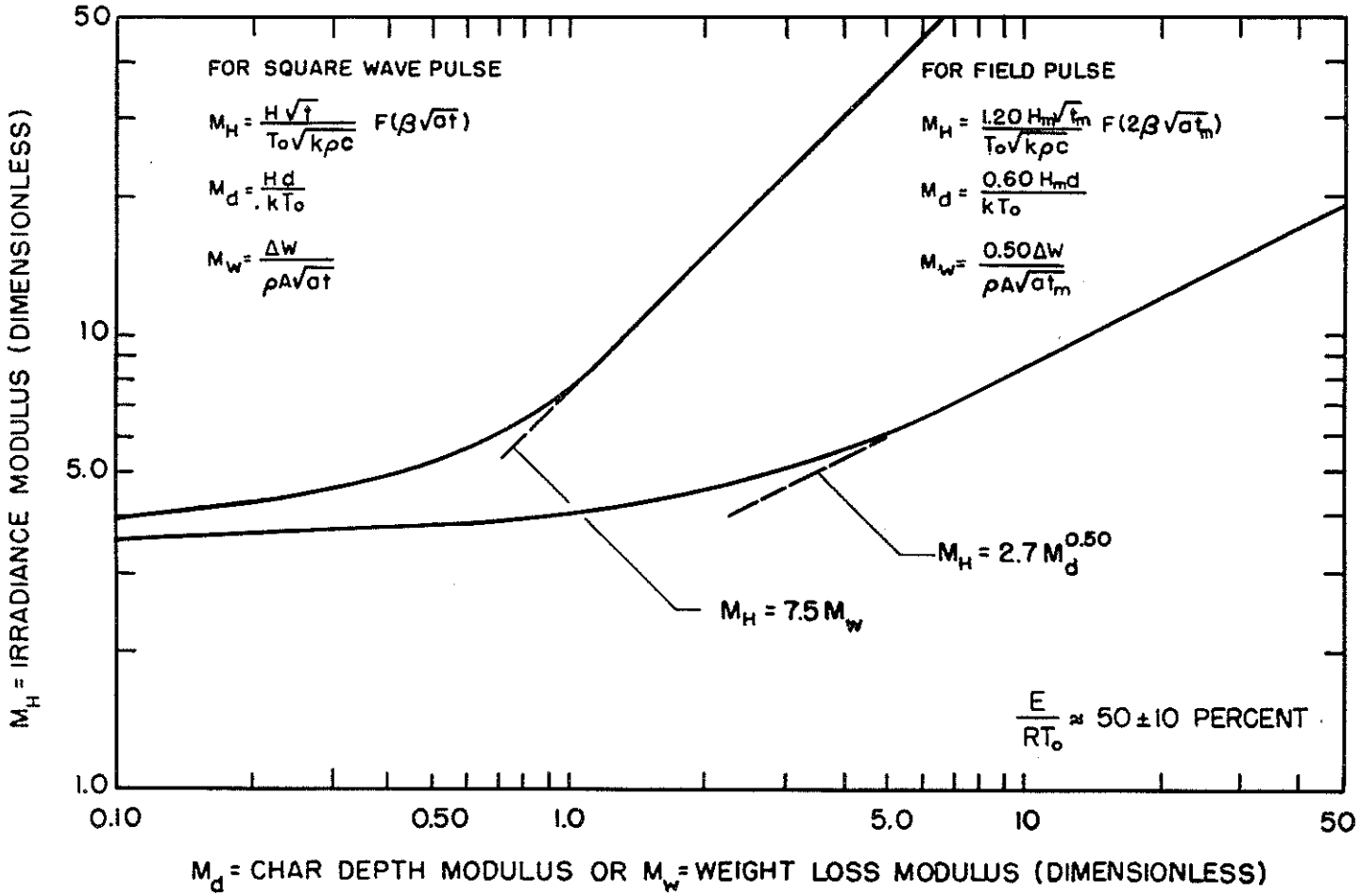

Figure 26.--Recommended correlations for depth of char and weight loss for semi-infinite solid. Radiant flux in the radial (normal to flat grain) direction, moisture content less than 8 percent, irradiance greater than 3 cal/cm^{2}sec, β = 100 cm^{-1}. Use 300°K for all T_o when 0 < T_o < 60°C. (N.B., for flux in the tangential direction, char depths 25 percent less than indicated.)

$$\left.\begin{aligned} \frac{c\Delta WT_o}{AH_m t_m} &= 0.32\ F(2\beta\sqrt{at_m}) \\ \frac{\rho c dT_o}{H_m t_m} &= 0.33\ F^2(2\beta\sqrt{at_m}) \end{aligned}\right\} \qquad (30)$$

and for the NRDL simulated field pulse[17/]

$$\left.\begin{aligned} \frac{c\Delta WT_o}{AQ_p} &= 0.15\ F(2\beta\sqrt{at_m}) \\ \frac{\rho c dT_o}{Q_p} &= 0.16\ F^2(2\beta\sqrt{at_m}) \end{aligned}\right\} \qquad (31)$$

The energy required for identical damage is 13 percent lower for the simulated field pulse compared with the square wave pulse. This difference is most probably within the accuracy of estimating the constants of equations (27) and (28). The pulse shape constants reported from field data (38, sheet 1a.1) vary considerably from that of the NRDL simulated field pulse. For this reason equation (30) is recommended over equation (31) until sufficient data have been gathered on charring produced by pulse shapes which deviate somewhat from the pulse shape constant of 2.08.

The reader has probably noticed the marked resemblance between the behavior of the proposed correlations and that proposed by Masters (10, sheet 4b.2) based on attainment of a maximum temperature. Both procedures have the following properties

$$\frac{\rho c dT}{Q} \simeq \text{constant}, \quad d \text{ large}$$

$$\frac{H\sqrt{t}}{T\sqrt{k\rho c}} \simeq \text{constant}, \quad d \text{ small}$$

17/ For the NRDL simulated field pulse p = 2.08.

the difference being in the specification of the temperature used during correlation. Since "charring" appears to take place rapidly over a limited range of temperature, (figure 3) Masters' criterion is somewhat correct and he is able to correlate depth of char data by choosing thermal properties which allow the data to fall on the proposed correlation. When steady state has been reached, the two correlation hypotheses are identical since the density gradient must have a 1:1 correspondence with a temperature gradient, however, not necessarily the one proposed by Masters. The author feels that the correlations proposed in this report are more basically correct and moreover lack the necessity of choosing thermal properties which differ from expected values.

CONCLUSIONS

Assuming that density variations within the irradiated semi-infinite solid follow a first order kinetic reaction, schematic integration of the differential equation yields dimensionless relationships between char depth and weight loss moduli and groupings representative of first, a rate-controlled process and secondly, a diffusion-controlled process. Analysis of NRDL depth of char and weight loss data leads to the conclusion that the latter process is controlling and should be used for correlation purposes.

Wood appears somewhat diathermanous even though the surface is charred. A second order correction for this effect improves the correlation. The absorption coefficient ($\beta_m = 100\ cm^{-1}$) was chosen to afford the best fit of the NRDL data.

The NRDL simulated field pulse data are correlated with corresponding square wave data through specification of an equivalent square wave pulse which has the characteristics

$$H\ (\text{square wave}) = 0.60\ H_m\ (\text{field pulse})$$

$$t\ (\text{square wave}) = 4.0\ t_m\ (\text{field pulse})$$

The equivalent square wave pulse results in satisfactory agreement of both depth of char and weight loss data over the entire range of variables tested.

Choice of thermal property values is discussed, and it appears that evaluation of properties on a dry basis afford the better correlation, at least for moisture contents less than 8 percent. More experimental data are necessary, however, to provide conclusive evidence as to quantitative effects of moisture. Additional experiments

must be run because previous work used various techniques to measure depth of char and there is some doubt that data from various experiments of this previous work are consistent.

MIT and NBS char depth measurements are approximately 25 percent lower, on a correlated basis, than the NRDL data. This differential appears to be associated with the direction of the radiant flux relative to the grain direction. NML static exposures result in large relative scatter of data which deviate from the expected trend at the greater depths of char. This deviation in NML data is ascribed to violation of the semi-infinite solid boundary condition although results are not conclusive on this point. NML dynamic exposures demonstrated large variations in the depth of char from the expected trend due to the effect of pulse shape.

Dimensionless correlation functions are presented for depth of char and weight loss which appear valid for irradiance levels greater than 3 $cal/cm^2 sec$ and for E/RT_o equal to 50 ± 10 percent. Estimating equations are derived for values of irradiance moduli greater than 7. In using correlation functions or equations it is suggested that T_o be taken as 300^oK for all initial temperatures in the range $0 \leqslant T_o \leqslant 60^oC$. For irradiance moduli greater than 7 "steady state" charring occurs, and depth of char and weight loss are approximately dependent on total energy delivered.

RECOMMENDATIONS

Due to the number of questions arising from the effects of grain orientation, finite thickness, moisture, and diathermancy, the author believes additional experimentation is justified before laboratory data may be applied to field conditions with the necessary degree of certainty. These investigations should be carried out by one agency primarily to insure that identical techniques are used throughout. At least two woods, whose densities differ as much as practicable, should be investigated. Note that moisture affects the thermal properties of less dense woods to the largest extent.

The apparent difference in grain orientation can be resolved by comparison of additional data on heart willow taken at right angles to the original direction. If this orientation shows the expected trend, remaining investigations should be carried out with the radiant flux tangential since this conforms to the usual grain orientation.

The effect of finite thickness is most perturbing and should be dispensed with before remaining parameters are investigated. The author suggests that the rear surface boundary condition be made isothermal, the most severe condition. By choosing various specimen thicknesses the value of d/L may be determined which causes deviation from the semi-infinite solid results.

The postulated effect of diathermancy can be checked by blackening the surface with india ink. If Gardon's results are correct, this should result in a nearly opaque solid for which $F(\beta\sqrt{at})$ approaches unity.

Variation of depth of char and weight loss with moisture should be investigated under ovendry conditions and double the value previously used (7-8 percent) provided heart willow remains one of the species tested. Due to the presented correlation procedure a large number of data will not be necessary. Data should, however, span the range of dimensionless moduli, care being taken to avoid violation of the semi-infinite solid condition.

In future work activation energies for each species investigated should be determined from isothermal weight loss data, especially if further investigation of the effect of initial temperature is contemplated. Particular attention should be given to resolving the difference observed between native species (i.e., heart willow) and tropical species (Guatemalan cedar).

LITERATURE CITED

1. Robertson, A. F.
   1952. Effects of geometry of flash thermal damage, WT-310. Operation BUSTER Proj. 2.3.

2. _____
   1954. Private communication dated November 3, 1954.

3. _____
   1951. Effects of thermal radiation on materials. Prog. Rept. 7. Natl. Bur. Stds.

4. _____
   1953. Effects of thermal radiation on materials (final report), AFSWP-281. Natl. Bur. Stds.

5. Laboratory Projects 5046-2 and 5046-3.
   1951. Thermal radiation studies, Prog. Rept. 3. Material Laboratory, N. Y. Naval Shipyard.

6. _____
   1952. Thermal radiation studies, Prog. Rept. 6, AFSWP-242. Material Laboratory, N. Y. Naval Shipyard.

7. Williams, C. C., III.
   1953. Damage initiation in organic materials exposed to high-intensity thermal radiation, Tech. Rept. 2. Fuels Res. Lab., Mass. Inst. Tech.

8. Robertson, A. F.
   1954. Private communication dated February 4, 1954.

9. Martin, S., Butler, C. P., and Plum, W. B.
   1954. Thermal radiation damage to cellulosic materials--Part I wood, AFSWP-796. U. S. Naval Radiological Defense Lab.

10. Masters, Joseph I.
    1953. A method for handling temperature dependent damage produced by short energy pulses irradiating semi-infinite solids, TO1, 53-9. Tech. Operations, Inc.

11. Lauwerier, H. A.
    1953. Optimum problems in the conduction of heat in a semi-infinite solid. Appl. Sci. Res., A, Vol. 4, 2. The Hague.

12. Bamford, C. H., Crank, J., and Malan, D. H.
1946. The combustion of wood--Part I. Proc. Cambridge Philos. Soc., XLII, pp. 166-182.

13. McNaughton, G. C.
1944. Ignition and charring temperatures of wood, R1464. U. S. For. Serv., Forest Products Lab. /mimeographed/

14. Wright, R. H., and Hayward, A. M.
1951. Kinetics of the thermal decomposition of wood. Can. J. Tech. 29(12): 503-510.

15. Stamm, A. J., Burr, H. K., and Kline, A. A.
1946. Stay b wood--Heat--stabilized wood. Indus. Eng. Chem. 38(6): 630.

16. MacLean, J. D.
1951. Rate of disintegration of wood under different heating conditions. Am. Wood Preservers Assn. 47: 155.

17. _____
1953. Effect of steaming on the strength of wood. Am. Wood Preservers Assn. 49: 88.

18. _____
1954. Effect of heating in water on the strength properties of wood. Am. Wood Preservers Assn. 50: 253.

19. _____
1955. Effect of oven heating and hot pressing on strength properties of wood. Am. Wood Preservers Assn. 51 /preprint/

20. Mitchell, R. L., Seborg, R. M., and Millet, M. A.
1953. Effect of heat on the properties of chemical composition of Douglas-fir wood and its major components. J. For. Prod. Res. Soc. 3: 38-42, 72-73.

21. Kujirai, Tsunetaro, and Akahira, Takeo
1925. Effect of temperature on the deterioration of fibrous insulating materials. Sci. Papers, Inst. Phys. Chem. Res. 2: 223-252.

22. Murphy, E. J.
1943. Gases evolved by the chemical decomposition of paper. Trans. Electrochemical Soc. 83: 161-174.

23. Klar, M.
The technology of wood distillation /trans. by A. Rule, London, 1925/, Chapt. III, p. 44.

24. Blanchard, Robert K.
1938. Progress report on fuel studies. U. S. For. Serv., Calif. For. Range Expt. Sta. /unpublished/

25. Stamm, A. J.
1955. Thermal degradation of wood and cellulose. Presented at 127th Natl. Meeting of the Am. Chem. Soc., Cincinnati, O.

26. MacLean, J. D.
1941. Thermal conductivity of wood. Heating, Piping and Air Conditioning 13(6): 380-91.

27. Dunlap, Frederick
1912. The specific heat of wood, For. Bul. 110. U. S. For. Serv.

28. Byram, G. M., and others
1952. Thermal properties of forest fuels, AFSWP-404. U. S. For. Serv., Div. Fire Res.

29. Wangaard, F. F.
1940. Transverse heat conductivity of wood. Heating, Piping and Air Conditioning 12(7): 459-464.

30. _____
1943. The effect of wood structure upon heat conductivity. Trans. Am. Soc. Mech. Eng. 65: 127-135.

31. Butler, C. P., and others
1953. The effect of pulse shape on thermal radiation damage to materials, AFSWP-478. U. S. Naval Radiological Defense Lab.

32. Carlslaw, H. S., and Jaeger, J. C.
1947. Conduction of heat in solids. Oxford Univ. Press, London.

33. Gardon, R.
1953. Temperatures attained in wood exposed in high intensity thermal radiation, Tech. Rept. 3. Fuels Res. Lab., Mass. Inst. Tech.

34. Raskin, W. H.
1953. Effects of thermal radiation on materials--eleventh progress report, AFSWP-280. Natl. Bur. Stds.

35. Khudyakov, G. N.
1951. /Distribution of temperature within a liquid burning from a free surface and description of the flame formed./ Izvestia Akademii Nauk, USSR No. 7, p. 1015. /In Russian. RAE Libr. Trans. No. 422, Royal Aircraft Est., Farnborough, England./

36. Petersen, E. E., Wright, C. C., and Walker, P. L., Jr.
1955. Reaction of artificial graphite with carbon dioxide. Ind. Eng. Chem. 47(8): 1624.

37. Broido, A., Butler, C. P., and Hillendahl, R. W.
1952. Basic thermal radiation measurements, WT-409. Operation BUSTER.

38. Armed Forces Special Weapons Project.
1954. Thermal radiation handbook, AFSWP-700.

39. Derkson, W. L., Bates, W. J., and Monahan, T. I.
1954. Research report on the use of polyethylene as a physical measuring system for evaluating physiological burns behind fabrics, AFSWP-834. Lab. Proj. 5046-3, Part 42, Final Report.

40. Schack, A.
1953. Der Industrielle warm eubergang /Industrial heat transfer/. 4th ed. Verlag Stahleisen m.b.H., Dusseldorf.

NOMENCLATURE

a	= thermal diffusivity	cm^2/sec
A	= surface area	cm^2
B	= a constant, the assumed value of ρ^+ at incipient charring	dimensionless
c	= specific heat	cal/gm (dry wood)^oC
Δc_p	= elevation of specific heat due to heat of desorption of bound water	cal/gm (dry wood)^oC
d	= depth of char measured from original surface	cm
E	= activation energy	kcal/mole
E^+	= E/RT_o	dimensionless
f	= weight fraction of inert material to dry wood	dimensionless
$F_o, F_1 \ldots\ldots F_n$	= functional relationships	
$G_o, G_1 \ldots\ldots G_n$	= functional relationships	
h	= heat transfer coefficient	$cal/cm^2 sec\,^oC$
H	= irradiance	$cal/cm^2 sec$
H^+	= $H\,t/\,k\rho c$	dimensionless
H_m	= maximum irradiance (second) for field pulse	$cal/cm^2 sec$
k	= thermal conductivity	$cal/cm^2 sec\,^oC/cm$
L	= thickness	cm
M	= moisture content	percent dry weight
P	= pulse shape factor = $\frac{Q_p}{H_m t_m}$	dimensionless
Q	= radiant energy	cal/cm^2
Q_p	= radiant energy of field pulse	cal/cm^2
R	= gas constant = 1.9864	$cal/mole\,^oK$
t	= square wave exposure time	sec
t_m	= time of second maximum for field pulse	sec
T	= absolute temperature	^oK
T_m	= maximum absolute surface temperature	^oK

T_o	= initial absolute temperature of specimen	^oK
ΔT	= $T - T_o$ = temperature rise	^oC
ΔT_s	= surface temperature rise	^oC
w	= fraction of decomposition products remaining in wood at time θ	dimensionless
w_o	= fraction of dry weight remaining at time θ	dimensionless
ΔW	= weight loss due to radiant exposure	gm
x	= position coordinate	cm
x^+	= $\alpha Hx/kT_o$	dimensionless
α	= surface absorptivity	dimensionless
β	= absorption coefficient	cm^{-1}
ϵ	= surface emissivity	dimensionless
η	= $x/2\sqrt{a\theta}$	dimensionless
η_1	= $x/2\sqrt{a(\theta-t)}$	dimensionless
η_2	= $x/2\sqrt{at}$	dimensionless
θ	= time	sec
μ	= velocity constant	sec^{-1}
μ^+	= $\mu x^2/2a$	dimensionless
ρ	= density at time θ	gm/cc
ρ_D	= density based on dry volume	gm/cc
ρ_M	= density based on volume at current moisture	gm/cc
ρ_o	= original density	gm/cc
ρ^+	= ρ/ρ_o	dimensionless
	= Stefan-Boltzmann constant = 1.37×10^{-12}	$cal/cm^2\ ^oK^4$